Observational test of inflation in loop quantum cosmology

Martin Bojowald[1], **Gianluca Calcagni**[2], **and Shinji Tsujikawa**[3]

[1] *Institute for Gravitation and the Cosmos, The Pennsylvania State University*
104 Davey Lab, University Park, PA 16802, U.S.A.
[2] *Max Planck Institute for Gravitational Physics (Albert Einstein Institute)*
Am Mühlenberg 1, D-14476 Golm, Germany
[3] *Department of Physics, Faculty of Science, Tokyo University of Science*
1-3, Kagurazaka, Shinjuku-ku, Tokyo 162-8601, Japan
E-mail: `bojowald@gravity.psu.edu`, `calcagni@aei.mpg.de`,
`shinji@rs.kagu.tus.ac.jp`

ABSTRACT: We study in detail the power spectra of scalar and tensor perturbations generated during inflation in loop quantum cosmology (LQC). After clarifying in a novel quantitative way how inverse-volume corrections arise in inhomogeneous settings, we show that they can generate large running spectral indices, which generally lead to an enhancement of power at large scales. We provide explicit formulas for the scalar/tensor power spectra under the slow-roll approximation, by taking into account corrections of order higher than the runnings. We place observational bounds on the inverse-volume quantum correction $\delta \propto a^{-\sigma}$ ($\sigma > 0$, a is the scale factor) and the slow-roll parameter ϵ_V for power-law potentials as well as exponential potentials by using the data of WMAP 7yr combined with other observations. We derive the constraints on δ for two pivot wavenumbers k_0 for several values of δ. The quadratic potential can be compatible with the data even in the presence of the LQC corrections, but the quartic potential is in tension with observations. We also find that the upper bounds on $\delta(k_0)$ for given σ and k_0 are insensitive to the choice of the inflaton potentials.

Contents

1. Introduction

Both the construction of quantum gravity and the question of its observational tests
are beset by a host of problems. On the one hand, quantum gravity, in whatever
approach, must face many mathematical obstacles before it can be completed to a
consistent theory. On the other hand, assuming that a consistent theory of quantum
gravity does exist, dimensional arguments suggest that its observational implications

are of small importance. In the realm of cosmology, for instance, they are estimated to be of the tiny size of the Planck length divided by the Hubble distance.

Between the two extremes of conceptual inconsistency and observational irrelevance lies a window of opportunity in which quantum gravity is likely to fall. It is true that we do not yet know how to make quantum gravity fully consistent, and it is true that its effects for early-universe cosmology should be expected to be small. But in trying to make some quantum-gravity modified cosmological equations consistent, it has been found that there can be stronger effects than dimensional arguments suggest. Consistency requirements, especially of loop quantum gravity, lead to modified spacetime structures that depart from the usual continuum, implying unexpected effects.

To partially bridge the gap between fundamental developments and loop quantum gravity phenomenology and observations, one considers effective dynamics coming from constraint functions evaluated on a particular background and on a large class of semiclassical states. In generally-covariant systems, the dynamics is fully constrained, and the constraint functionals on phase space generate gauge transformations obeying an algebra that reveals the structure of spacetime deformations. The algebra of these gauge generators thus shows what underlying notion of spacetime covariance is realized, or whether covariance might be broken by quantum effects, making the theory inconsistent. If a consistent version with an unbroken (but perhaps deformed) gauge algebra exists, it can be evaluated for potential observational implications.

These effective constraints and their algebra, at the present stage of developments, can be evaluated for perturbative inhomogeneities around a cosmological background. While loop quantum gravity is background independent in the sense that no spacetime metric is assumed before the theory is quantized, a background and the associated perturbation theory can be introduced at the effective level. In the case of interest here, the background is cosmological, a flat Friedmann–Robertson–Walker (FRW) spacetime with a rolling scalar field and perturbed by linear inhomogeneous fluctuations of the metric-matter degrees of freedom. The idea is to implement as many quantum corrections as possible, and study how the inflationary dynamics is modified. In this context, it is important that no gauge fixing be used before quantization, as such a step would invariably eliminate important consistency conditions by fiat, not by solving them. The result would be a framework whose "predictions" depend on how the gauge was fixed in the first place.

This program, challenging as it is, has been carried out only partially so far, and in gradual steps. First, the full set of constraints was derived for vector [1], tensor [2], and scalar modes [4, 5] in the presence of small inverse-volume corrections. The gravitational wave spectra have been studied in [6, 7], where the effect of inverse-volume corrections and their observability were discussed. The scalar inflationary spectra and the full set of linear-order cosmological observables was then derived in

[8], thus making it possible to place observational bounds on the quantum corrections themselves [9] (see also Refs. [10] for early related works). The reason why these studies concentrate on inverse-volume corrections is mainly technical; in fact, the closure of the constraint algebra has been verified only in this case (and only in the limit of small corrections). A class of consistent constraints with a closed algebra is known also for vector and tensor modes in the presence of holonomy corrections [1, 2, 3], but it remains unknown what set of constraints, if any, can be consistent in the scalar sector, where anomaly cancellation is more difficult to work out [11]. Therefore, inspections of cosmological holonomy effects have been so far limited to the tensor sector [6, 12, 13].

Exactly isotropic minisuperspace models, where the situation is reversed and holonomy corrections are easier to implement than inverse-volume corrections, provide another reason why it is interesting to focus attention on inverse-volume corrections. Effective equations available for certain matter contents with a dominating kinetic energy [14, 15] suggest that holonomy corrections are significant only in regimes of near-Planckian densities [16] but not during the timespan relevant for early-universe cosmology, including inflation. Inverse-volume corrections, on the other hand, do not directly react to the density but rather to the discreteness scale of quantum gravity, which is not determined immediately by the usual cosmological parameters. The question of whether they are small or can play a significant role must be answered by a self-consistent treatment.

Such a treatment shows that inverse-volume corrections present an example of quantum-gravity effects that can be larger than what dimensional arguments suggest [9]. Here we present the full details of the analysis briefly reported in [9] for a quadratic inflationary potential, enriching it with new constraints on other potentials. From a cosmological perspective, we shall provide the complete set of slow-roll equations as functions of the potential, extend the likelihood analysis to quartic and exponential potentials, and discuss how the experimental pivot scale and cosmic variance affect the results.

Before examining the details and experimental bounds of the model, from a quantum-gravity perspective we will clarify some conceptual issues which must be taken into account for a consistent treatment of inverse-volume corrections. In particular, we justify for the first time why inverse-volume corrections depend only on triad variables, and not also on connections. Until now, this was regarded as a technical assumption devoid of physical motivations. Here we show it as a consequence of general but precise semiclassical arguments. Further, we spell the reason why inverse-volume corrections are not suppressed at the inflationary density scale.

The plan of the paper is as follows. We begin in section 2 by discussing inverse-volume corrections in LQC and their justification in inhomogeneous models, providing the first implementation for a class of semiclassical states sufficiently large to be used in effective equations. After this section, we turn to an application for

observational cosmology. In section 3.1 we review the formulas of the cosmological observables in the Hubble slow-roll tower [8]. In section 3.2 we reexpress these quantities in the slow-roll parameters as functions of the inflationary potential. In section 4 the observables are recast as functions of the momentum pivot scale for a ready use in numerical programs. The effect of cosmic variance on the scalar power spectrum is also discussed therein. In section 5 we shall carry out the likelihood analysis to constrain the inverse-volume corrections in the presence of several different inflaton potentials by using the observational data of Cosmic Microwave Background (CMB) combined with other datasets.

2. Cosmology with a discrete scale

One of the main features of loop quantum gravity (LQG), shared with other approaches to quantum gravity, is the appearance of discrete spatial structures replacing the classical continuum of general relativity. It is often expected that the scale of the discreteness is determined by the Planck length $\ell_{\rm Pl} = \sqrt{G\hbar}$, but if discreteness is fundamental, its scale must be set by a dynamical parameter of some underlying state, just as the lattice spacing of a crystal is determined by the interaction of atoms. In this section, we develop the cosmological picture of dynamics of discrete space, highlighting the form of quantum corrections to be expected. Readers more interested in potentially observable consequences may skip this technical part, but those acquainted with LQC will find a fresh discussion and justification of inverse-volume corrections and the lattice refinement picture.

In loop quantum gravity, such states are represented by spin networks, graphs in an embedding space whose edges e are labeled by spin quantum numbers j_e. The quantum number determines the area of an elementary plaquette intersecting only one edge e, given by $\mathcal{A} = \gamma \ell_{\rm Pl}^2 \sqrt{j_e(j_e + 1)}$. As the plaquette is enlarged, its geometrical size changes only when it begins to intersect another edge, increasing in quantum jumps. In the area formula, γ is the Barbero–Immirzi parameter, whose size (slightly less than one) can be inferred from computations of black-hole entropy [17, 18]. As expected, the scale is set by the Planck length for dimensional reasons, but the actual size is given by the spin quantum number. Its values in a specific physical situation have to be derived from the LQG dynamical equations, a task which remains extremely difficult. However, given the form in which j_e appears in the dynamical equations, its implications for physics can be traced and parametrized in sufficiently general form so as to analyze effects phenomenologically.

2.1 Scales

In order to model this situation in general terms, we begin with a nearly isotropic spacetime and a chunk of space of some comoving size $\mathcal{V}_0$, as measured by the extensions in some set of coordinates. The geometrical size is then $\mathcal{V} = \mathcal{V}_0 a^3$, where

a is the scale factor. We complement this classical picture with a discrete quantum picture, in which the same chunk of space is made up from nearly-isotropic discrete building blocks, all of the same size v. If there are $\mathcal{N}$ discrete blocks in a region of size $\mathcal{V}$, we have the relationship $v = \mathcal{V}_0 a^3 / \mathcal{N}$. The elementary volume v, or the linear scale $L = v^{1/3}$, will be our main parameter, related to the quantum state via its labels j_e. The elementary quantum-gravity scale L need not be exactly the Planck length, depending on what j_e are realized. Instead of using the j_e, which are subject to complicated dynamics, it turns out to be more useful to refer to L in phenomenological parametrizations. Similarly, we define the quantum-gravity density scale

$$\rho_{\mathrm{QG}} = \frac{3}{8\pi G L^2} \,, \tag{2.1}$$

which equals $3/8\pi$ times the Planck density for $L = \ell_{\mathrm{Pl}}$.

In loop quantum gravity, the discreteness is mathematically seen as a rather direct consequence of the fact that the fundamental operators are holonomies along curves e, computed for a certain form of gravitational connection, the Ashtekar–Barbero connection A_a^i,[1] while the connection itself is not a well-defined operator. For a nearly isotropic spacetime, there is only one nontrivial connection component, given by $c = \gamma \dot{a}$ in terms of the proper-time derivative of the scale factor. The classical holonomies are $h_e = \mathcal{P} \exp(\int_e \mathrm{d}\lambda\, \dot{e}^a A_a^i \tau_i)$, with $\tau_j = \mathrm{i}\sigma_j/2$ proportional to Pauli matrices and path ordering indicated by $\mathcal{P}$. Every h_e takes values in the compact group $\mathrm{SU}(2)$, whose representations appear as the spin labels of edges j_e, giving rise to discrete conjugate variables.

Another consequence of one being able to represent only holonomies, not connection components, is that the usual polynomial terms in connection-dependent Hamiltonians are replaced by the whole series obtained by expanding the exponential expression for an holonomy. In this way, higher-order corrections are implemented in the dynamics. Corrections become significant when the argument of holonomies, given by line integrals of A_a^i along the spin-network edges, is of order one. For a nearly isotropic connection $A_a^i = c\delta_a^i$, the integral along straight lines reduces to $\ell_0 c$, where ℓ_0 is the coordinate (i.e., comoving) length of the edge. If the edge is elementary and of the discreteness size of our underlying state, we have $\ell_0 = L/a = v^{1/3}/a$, and the condition for holonomy corrections becoming large is $v^{1/3}c/a \sim 1$. More intuitively, holonomy corrections become large when the Hubble scale $H^{-1} = a/\dot{a} \sim \gamma L$ is of the size of the discreteness scale, certainly an extreme regime in cosmology. Yet another intuitive way of expressing this regime is via densities: holonomy corrections are large when the matter density is of the order of the quantum-gravity density. By the classical Friedmann equation, this happens when

$$\rho = \frac{3}{8\pi G} H^2 = \frac{3}{8\pi G} \frac{c^2}{a^2 \gamma^2} \sim \frac{3}{8\pi G \gamma^2 L^2} = \gamma^{-2} \rho_{\mathrm{QG}} \,. \tag{2.2}$$

---

[1] Indices $a, b, \dots = 1, 2, 3$ run over space directions, while $i, j, \dots = 1, 2, 3$ are internal indices in the su(2) algebra.

We introduce the parameter $\delta_{\mathrm{hol}} := \rho/\rho_{\mathrm{QG}} = 8\pi G v^{2/3}\rho/3$ in order to quantify holonomy corrections. These are small when $\delta_{\mathrm{hol}} \ll 1$.

The discreteness of loop quantum gravity manifests itself in different ways, some of which require more details to be derived. In addition to holonomy corrections, the most important one arises when one considers the inverse of the elementary lattice areas. Classically, the areas correspond to the densitized triad E_i^a, which determines the spatial metric q_{ab} via $E_i^a E_i^b = q^{ab} \det q$ and is canonically conjugate to the connection A_a^i. The inverse of E_i^a or its determinant appears in the Hamiltonian constraint of gravity as well as in all the usual matter Hamiltonians, especially in kinetic terms, and is thus crucial for the dynamics.

Upon quantization, however, the densitized triad is represented in terms of the spin labels that also determine the lattice areas, and those labels can take the value zero. No densely defined inverses of the area operators exist, and therefore there is no direct way to quantize inverse triads or inverse volumes as they appear in Hamiltonians. However, as with holonomies replacing connection components, there is an indirect way of constructing well-defined inverse-volume operators, which imply further quantum corrections.

2.2 Derivation of inverse-volume corrections

The quantization of different kinds of inverse volumes or the co-triad e_a^i, obtained from the inverse of E_i^a, begins with Poisson identities such as [19, 20]

$$\left\{A_a^i, \int \mathrm{d}^3x\sqrt{|\det E|}\right\} = 2\pi\gamma G\epsilon^{ijk}\epsilon_{abc}\frac{E_j^b E_k^c}{\sqrt{|\det E|}}\,\mathrm{sgn}(\det E) = 4\pi\gamma Ge_a^i\,, \qquad (2.3)$$

stemming from the basic Poisson brackets $\{A_a^i(x), E_j^b(y)\} = 8\pi G\gamma\delta_j^i\delta_a^b\delta(x,y)$. On the right-hand side of Eq. (2.3), there is an inverse of the determinant of E_i^a, but on the left-hand side no such inverse is required. Classically, the inverse arises from derivatives contained in the Poisson bracket, but after quantization the Poisson bracket is replaced by a commutator and no derivative or inverse appears. In this way, one obtains well-defined operators for the inverse volume, implementing an automatic ultraviolet cutoff at small length scales.

The volume $\int \mathrm{d}^3x\sqrt{|\det E|}$ of some region, containing the point v where we want to evaluate the co-triad, is quantized by well-defined volume operators, and the connection can be represented in terms of holonomies. For holonomies with edges of comoving length ℓ_0, we can write

$$\mathrm{tr}(\tau^i h_{\mathrm{v},e}[h_{\mathrm{v},e}^{-1}, \hat{V}_{\mathrm{v}}]) \sim \frac{1}{2}\mathrm{i}\hbar\ell_0\{\widehat{A_a^i, V_{\mathrm{v}}}\}\dot{e}^a\,. \qquad (2.4)$$

Here, $\tau^j = \mathrm{i}\sigma^j/2$ are Pauli matrices, $h_{\mathrm{v},e}$ is a holonomy starting at a lattice vertex v in some direction e, and V_{v} is the volume of some region around v, with $\hat{V}_{\mathrm{v}}$ its quantization. As long as v is included in the region integrated over to obtain the

volume, it does not matter how far the region extends beyond v. One could even use the volume of the whole space.

To quantize, loop quantum gravity provides the holonomy-flux representation of the basic operators $\hat{h}_{v,e}$ (holonomies along edges e) and $\hat{F}_S = \int_S d^2y\, E_i^a n_a$, fluxes of the densitized triad through surfaces S with co-normal n_a. These variables are SU(2)-valued, but one can devise a regular lattice for a simple implementation of inhomogeneity, setting edges with tangent vectors $\dot{e}_I^a = \delta_I^a$, $I = 1, 2, 3$ in Cartesian coordinates. Then, holonomies are given by $h_{v,e_I} = \exp(\ell_0 \tau_I c) = \cos(\ell_0 c/2) + 2\tau_I \sin(\ell_0 c/2) \in$ SU(2), where c is the connection evaluated somewhere on the edge. All connection-dependent matrix elements can thus be expressed in the complete set of functions $\eta := \exp(i\ell_0 c/2) \in$ U(1), and the flux through an elementary lattice site in a nearly isotropic geometry is simply $F = \ell_0^2 p$ with $|p| \sim a^2$, and p carrying a sign amounting to the orientation of space. Isotropy thus allows a reduction from SU(2) to U(1), with certain technical simplifications.

For a nearly isotropic configuration, we assign a copy of the isotropic quantum theory to every (oriented) link I of a regular graph, making the theory inhomogeneous. By this step we certainly do not reach the full theory of loop quantum gravity, which is based on irregular graphs with SU(2)-theories on its links. But we will be able to capture the main effects which have appeared in approximate considerations of loop quantum gravity with simpler graphs and reduced gauge groups. The basic operators are then a copy of $\hat{\eta}_{v,I}$ and $\hat{F}_{v,I}$ for each lattice link with

$$[\hat{\eta}_{v,I}, \hat{F}_{v',J}] = -4\pi\gamma\ell_{\mathrm{Pl}}^2 \hat{\eta}_{v,I} \delta_{IJ} \delta_{v,v'}, \tag{2.5}$$

if the edge of the holonomy and the surface of the flux intersect.

When we insert holonomies for nearly isotropic connections in Eq. (2.4) and evaluate the trace, inverse-volume operators resulting from commutators have the form

$$\hat{B}_{v,I} = \frac{1}{4\pi\gamma G\hbar} \left(\hat{\eta}_{v,I}^\dagger \hat{V}_v \hat{\eta}_{v,I} - \hat{\eta}_{v,I} \hat{V}_v \hat{\eta}_{v,I}^\dagger \right). \tag{2.6}$$

The volume at vertex v is obtained from components of the densitized triad, quantized by a flux operator $\hat{F}_{v,I}$, with v an endpoint of the link I. If (I, I', I'') denotes the triple of independent links emanating from a given vertex, we can write the volume as $\hat{V}_v = \sqrt{|\hat{F}_{v,I}\hat{F}_{v,I'}\hat{F}_{v,I''}|}$. Thus,

$$\hat{B}_{v,I} = \frac{1}{4\pi\gamma G\hbar} \left(\hat{\eta}_{v,I}^\dagger \sqrt{|\hat{F}_{v,I}\hat{F}_{v,I'}\hat{F}_{v,I''}|} \hat{\eta}_{v,I} - \hat{\eta}_{v,I} \sqrt{|\hat{F}_{v,I}\hat{F}_{v,I'}\hat{F}_{v,I''}|} \hat{\eta}_{v,I}^\dagger \right). \tag{2.7}$$

As in the general representation, the basic operators $\hat{F}_{v,I}$ and $\hat{\eta}_{v,I}$ satisfy the commutator identity (2.5) while $\hat{\eta}_{v,I}$ commutes with $\hat{F}_{v,I'}$ and $\hat{F}_{v,I''}$. Moreover, $\hat{\eta}_{v,I}$ satisfies the reality condition $\hat{\eta}_{v,I}\hat{\eta}_{v,I}^\dagger = 1$. It turns out that these identities are sufficient to derive the form of inverse-triad corrections in a semiclassical expansion, irrespective of what state is used beyond general requirements of semiclassicality.

We consider the two operators $\hat{\eta}_{\mathrm{v},I}|\hat{F}_{\mathrm{v},I}|^{1/2}\hat{\eta}_{\mathrm{v},I}^{\dagger}$ and $\hat{\eta}_{\mathrm{v},I}^{\dagger}|\hat{F}_{\mathrm{v},I}|^{1/2}\hat{\eta}_{\mathrm{v},I}$ separately.[2] They can be simplified using the basic commutators (2.5) and $[\hat{\eta}_{\mathrm{v},I}^{\dagger}, \hat{F}_{\mathrm{v},I}] = 4\pi\gamma\ell_{\mathrm{Pl}}^{2}\hat{\eta}_{\mathrm{v},I}^{\dagger}$. We can thus reorder terms so as to bring $\hat{\eta}_{\mathrm{v},I}$ right next to $\hat{\eta}_{\mathrm{v},I}^{\dagger}$, and then cancel them using the reality condition. Reordering according to $\hat{\eta}_{\mathrm{v},I}\hat{F}_{\mathrm{v},I} = (\hat{F}_{\mathrm{v},I} - 4\pi\gamma\ell_{\mathrm{Pl}}^{2})\hat{\eta}_{\mathrm{v},I}$ and $\hat{\eta}_{\mathrm{v},I}^{\dagger}\hat{F}_{\mathrm{v},I} = (\hat{F}_{\mathrm{v},I} + 4\pi\gamma\ell_{\mathrm{Pl}}^{2})\hat{\eta}_{\mathrm{v},I}^{\dagger}$ leads to

$$\hat{\eta}_{\mathrm{v},I}|\hat{F}_{\mathrm{v},I}|^{1/2}\hat{\eta}_{\mathrm{v},I}^{\dagger} = |\hat{F}_{\mathrm{v},I} - 4\pi\gamma\ell_{\mathrm{Pl}}^{2}|^{1/2}, \qquad \hat{\eta}_{\mathrm{v},I}^{\dagger}|\hat{F}_{\mathrm{v},I}|^{1/2}\hat{\eta}_{\mathrm{v},I} = |\hat{F}_{\mathrm{v},I} + 4\pi\gamma\ell_{\mathrm{Pl}}^{2}|^{1/2}. \quad (2.8)$$

In the classical limit $\hbar \to 0$, these expressions in $\hat{B}_{\mathrm{v},I}$ result in a derivative by $F_{\mathrm{v},I}$, as required by the Poisson bracket relationship (2.3). For inverse-volume effects we are interested in the leading quantum corrections with $\hbar \neq 0$, which arise in different forms. First, because the operator is nonlinear in the basic ones $\hat{F}_{\mathrm{v},I}$ and $\hat{\eta}_{\mathrm{v},I}$, classical expressions will be corrected by terms involving the moments of a state: As always in quantum physics, the expectation value $\langle\hat{B}_{\mathrm{v},I}\rangle$ does not have the classically expected relationship with expectation values of the basic operators. We can compute these corrections by following the principles of canonical effective dynamics, substituting $\langle\hat{F}_{\mathrm{v},I}\rangle + (\hat{F}_{\mathrm{v},I} - \langle\hat{F}_{\mathrm{v},I}\rangle)$ for $\hat{F}_{\mathrm{v},I}$ and performing a formal expansion by $\hat{F}_{\mathrm{v},I} - \langle\hat{F}_{\mathrm{v},I}\rangle$:

$$\hat{\eta}_{\mathrm{v},I}|\hat{F}_{\mathrm{v},I}|^{1/2}\hat{\eta}_{\mathrm{v},I}^{\dagger} = |\hat{F}_{\mathrm{v},I} - 4\pi\gamma\ell_{\mathrm{Pl}}^{2}|^{1/2}$$
$$= |\langle\hat{F}_{\mathrm{v},I}\rangle - 4\pi\gamma\ell_{\mathrm{Pl}}^{2}|^{1/2} \sum_{k=0}^{\infty} \binom{1/2}{k} \frac{(\hat{F}_{\mathrm{v},I} - \langle\hat{F}_{\mathrm{v},I}\rangle)^{k}}{|\langle\hat{F}_{\mathrm{v},I}\rangle - 4\pi\gamma\ell_{\mathrm{Pl}}^{2}|^{k}}, \qquad (2.9)$$

$$\hat{\eta}_{\mathrm{v},I}^{\dagger}|\hat{F}_{\mathrm{v},I}|^{1/2}\hat{\eta}_{\mathrm{v},I} = |\hat{F}_{\mathrm{v},I} + 4\pi\gamma\ell_{\mathrm{Pl}}^{2}|^{1/2}$$
$$= |\langle\hat{F}_{\mathrm{v},I}\rangle + 4\pi\gamma\ell_{\mathrm{Pl}}^{2}|^{1/2} \sum_{k=0}^{\infty} \binom{1/2}{k} \frac{(\hat{F}_{\mathrm{v},I} - \langle\hat{F}_{\mathrm{v},I}\rangle)^{k}}{|\langle\hat{F}_{\mathrm{v},I}\rangle + 4\pi\gamma\ell_{\mathrm{Pl}}^{2}|^{k}}. \qquad (2.10)$$

(This expansion can be made well-defined and analyzed in the context of Poisson geometry of algebraic state spaces [21, 22, 23].)

All terms in $\hat{F}_{\mathrm{v},I} - \langle\hat{F}_{\mathrm{v},I}\rangle$ will either vanish upon taking an expectation value ($k = 1$ in the expansion) or give rise to moments of the quantum state used to compute the expectation value ($k \geq 2$, with fluctuations and correlations arising for $k = 2$). The precise values of the moments and their dynamics depend on the state used and in fact encode the state dependence of the theory, but for a semiclassical state they satisfy, by definition, the hierarchy $\langle(\hat{F}_{\mathrm{v},I} - \langle\hat{F}_{\mathrm{v},I}\rangle)^{k}\rangle \sim \hbar^{k/2}$. This notion of semiclassicality is a very general one; it does not require us to choose a particular shape of the state, such as a Gaussian.

The moment terms imply an important form of quantum corrections in the context of quantum back-reaction. Such corrections arise from different sources in the Hamiltonians, which will all have to be combined and analyzed. We will not enter

---

[2]The factors of $\sqrt{|\hat{F}_{\mathrm{v},I'}|}$ and $\sqrt{|\hat{F}_{\mathrm{v},I''}|}$ quantize positive powers of the densitized triad and do not give rise to inverse-volume corrections.

such an analysis here, but rather note that even if we disregard quantum back-reaction, quantum corrections do remain: we have

$$\frac{1}{4\pi\gamma G\hbar}(\hat{\eta}_{\mathrm{v},I}^{\dagger}|\hat{F}_{\mathrm{v},I}|^{1/2}\hat{\eta}_{\mathrm{v},I} - \hat{\eta}_{\mathrm{v},I}|\hat{F}_{\mathrm{v},I}|^{1/2}\hat{\eta}_{\mathrm{v},I}^{\dagger})$$
$$= \frac{|\langle\hat{F}_{\mathrm{v},I}\rangle + 4\pi\gamma\ell_{\mathrm{Pl}}^{2}|^{1/2} - |\langle\hat{F}_{\mathrm{v},I}\rangle - 4\pi\gamma\ell_{\mathrm{Pl}}^{2}|^{1/2}}{4\pi\gamma\ell_{\mathrm{Pl}}^{2}} + \cdots, \qquad (2.11)$$

where the dots indicate moment terms dropped. This expression includes inverse-volume corrections, computed for general semiclassical states. It matches with ex-pressions derived directly from triad eigenstates [24, 25], which are not semiclassical but, as proven here, provide reliable information about inverse-volume corrections. More general semiclassical states do not introduce additional dependence of inverse-volume corrections on connection components or curvature, they just introduce moment terms which contribute to quantum back-reaction. (Such an extra dependence may arise from non-Abelian properties of the theory [26], which are not strong for perturbative inhomogeneities.)

2.3 Correction functions

Corrections to classical Hamiltonians in which inverse triad components appear can be captured by introducing correction functions such as

$$\alpha(a) := \frac{|L(a)^2 + 4\pi\gamma\ell_{\mathrm{Pl}}^{2}|^{1/2} - |L(a)^2 - 4\pi\gamma\ell_{\mathrm{Pl}}^{2}|^{1/2}}{4\pi\gamma\ell_{\mathrm{Pl}}^{2}} L(a), \qquad (2.12)$$

obtained by identifying

$$\langle\hat{F}_{\mathrm{v},I}\rangle = L^2(a) \qquad (2.13)$$

with the discreteness scale (depending on the scale factor in the presence of lattice refinement [8]). The multiplication of inverse-volume corrections by $L(a)$ ensures that $\alpha(a) \sim 1$ in the classical limit, but strong corrections can arise for small L. Our derivations apply to small deviations from the classical value, for which consistent implementations in the dynamics are available. We can thus expand

$$\alpha(a) = 1 + \alpha_0\delta_{\mathrm{Pl}} + \cdots, \qquad (2.14)$$

with $\delta_{\mathrm{Pl}} := (\ell_{\mathrm{Pl}}/L)^m$ for $m = 4$ in the above derivation, and the dots indicating powers higher than m.

For $\langle\hat{F}_{\mathrm{v},I}\rangle \gg \ell_{\mathrm{Pl}}^{2}$ inverse-volume corrections become very small, but they are significant if $\langle\hat{F}_{\mathrm{v},I}\rangle$ is about as large as a Planck area or smaller. Bringing in our discreteness scale, leading inverse-volume corrections can be expressed in terms of the quantity

$$\delta_{\mathrm{Pl}} = \left(\frac{\ell_{\mathrm{Pl}}}{L}\right)^4 = \left(\frac{\ell_{\mathrm{Pl}}^{3}}{v}\right)^{\frac{4}{3}} \qquad (2.15)$$

(using $m = 4$ from now on). If L or v is constant, δ_{Pl} is constant and inverse-volume corrections merely amount to rescaling some expressions in Hamiltonians. More generally, however, the dynamical nature of a discrete state suggests that L and v change in time or, in cosmology, with respect to the scale factor a. We parameterize this dependence as

$$\delta_{\mathrm{Pl}} \propto a^{-\sigma} \tag{2.16}$$

with $\sigma \geq 0$; see [8] for a discussion of possible values of σ and its relation to quantization parameters.

In order to compare inverse-volume with holonomy corrections, we write

$$\delta_{\mathrm{Pl}} = \left(\frac{8\pi G}{3}\rho_{\mathrm{QG}}\ell_{\mathrm{Pl}}^2\right)^2 = \left(\frac{8\pi}{3}\frac{\rho_{\mathrm{QG}}}{\rho_{\mathrm{Pl}}}\right)^2 = \left(\frac{8\pi}{3}\frac{\rho}{\rho_{\mathrm{Pl}}}\delta_{\mathrm{hol}}^{-1}\right)^2. \tag{2.17}$$

The second equality shows that inverse-volume corrections are considerable and of the order one when the quantum-gravity density is close to the Planck density. Inverse-volume corrections thus behave very differently from what is normally expected for quantum gravity, where the Planck density is often presupposed as the quantum-gravity scale. In loop quantum gravity, this scale must be sufficiently small compared to the Planck density in order to be consistent with inverse-volume corrections.

The last expression in Eq. (2.17) is useful in order to compare holonomy with inverse-volume corrections. Inverse-volume corrections are usually suppressed by a factor of ρ/ρ_{Pl}, as expected for quantum-gravity effects, but there is an extra factor of $\delta_{\mathrm{hol}}^{-1}$. For small densities, holonomy corrections are small, but inverse-volume corrections may still be large because they are magnified by the inverse of δ_{hol}. As the energy density decreases in an expanding universe, holonomy corrections fall to small values, and in this way begin to magnify inverse-volume corrections. For instance, in an inflationary regime with a typical energy scale of $\rho \sim 10^{-10}\rho_{\mathrm{Pl}}$, we can use (2.17) to write $\delta_{\mathrm{hol}} \sim 10^{-9}/\sqrt{\delta_{\mathrm{Pl}}}$. Having small holonomy corrections of size $\delta_{\mathrm{hol}} < 10^{-6}$ then requires inverse-volume correction larger than $\delta_{\mathrm{Pl}} > 10^{-6}$. This interplay of holonomy and inverse-volume corrections makes loop quantum gravity testable because it leaves only a finite window for consistent parameter values, rather than just providing Planckian upper bounds. It also shows that inverse-volume corrections become dominant for sufficiently small densities, as they are realized even in high-energy scenarios of inflation.

In this context, it is worthwhile to comment on a comparison of the corrections derived here, assuming a nearly isotropic but explicitly inhomogeneous discrete state, with their form in pure minisuperspace quantizations. In inverse-volume as well as holonomy corrections, we referred to elementary building blocks of a discrete state, the plaquette areas in inverse-volume corrections and edge lengths in holonomy corrections. A pure minisuperspace quantization would primarily make use of macroscopic parameters such as the volume of some region (or the scale factor). The

number of discrete blocks, such as $\mathcal{N}$ introduced above, is not available, and thus it is more difficult to refer to local microscopic quantities such as $F_{\mathrm{v},I}$.

For curvature or the Hubble parameter, local quantities are easier to introduce and to use in holonomy corrections, but inverse-volume expressions must refer to quantities of size, which cannot be expressed microscopically in a pure minisuperspace context. As a consequence, inverse-volume corrections have often been misrepresented in loop quantum cosmology. Without referring to $\mathcal{N}$, as it is introduced in the lattice-refinement formulation of loop quantum cosmology, one can only use the macroscopic volume of some region instead of the microscopic $F_{\mathrm{v},I}$.[3] Inverse-volume corrections become smaller for larger $F_{\mathrm{v},I}$, and thus substituting this quantity by a macroscopic size suppresses the corrections. Any such suppression is merely an artifact of using the wrong expressions for the corrections based solely on minisuperspace considerations. Using a macroscopic volume also makes the corrections dependent on the size of the chosen region, which is another artificial dependence on extra parameters; because of this, LQC inverse-volume corrections have been often interpreted as problematic or even unphysical. The derivation shown here solves these problems; see also the following subsection.

As already seen, inverse-volume corrections show unexpected properties in terms of their dependence on the density, and regimes in which they are strong. Another unexpected property is seen in their influence on spacetime structure, with important consequences for cosmological perturbation theory. Inverse-volume corrections are not just of higher-curvature type in an effective action, but they deform the usual gauge algebra of generally covariant systems, generating spacetime diffeomorphisms. This deformation, as discussed in more detail in the following calculations, leads to characteristic cosmological effects. In a conceptual context, moreover, it allows us to distinguish inverse-volume corrections from the other types encountered in loop quantum gravity: holonomy corrections and quantum back-reaction.

A closer look at the algebra of constraints generating the gauge transformations reveals that deformations of the algebra introduced by inverse-volume corrections cannot be undone by including holonomy corrections or quantum back-reaction [8]. Holonomy corrections imply higher-order terms in the constraints depending on the connection nonpolynomially, or at least on the background connection if an expansion by inhomogeneities is done. No such terms arise for inverse-volume corrections, and no cancellation is possible. Quantum back-reaction, on the other hand, comes from terms including moments of a state, as alluded to in our derivation of inverse-volume corrections. The dependence on the moments remains if one computes the constraint

---

[3]As mentioned earlier, in the inhomogeneous theory we can use the full volume or the size of any region in inverse-volume corrections because most plaquette contributions, which do not intersect the edge of the holonomies used, drop out. In homogeneous models, on the other hand, all plaquettes are equivalent and correspond to the same degree of freedom. The choices must thus be specified carefully in order to avoid minisuperspace artifacts.

algebra, in such a way that corrections from quantum back-reaction cannot cancel deformations implied by inverse-volume corrections, either. Since the characteristic effects analyzed here are a consequence of nontrivial deformations of the algebra, we can safely conclude that including only inverse-volume corrections does give a reliable picture, because they cannot be cancelled by the other, more complicated corrections. Of course, it remains of interest to study the inclusion of other effects such as the curvature of the universe, and the simultaneous competition between inverse-volume and other quantum corrections in a more complete dynamical analysis.

2.4 Consistency

Most of the properties and consequences of inverse-volume corrections are unexpected and unfamiliar. It is then perhaps not surprising that there are at least four main objections to the physical significance of effective LQC dynamics with inverse-volume corrections, which are popularly encountered in the literature and in scientific debates. It is claimed that (i) these corrections are ill-defined in a pure minisuperspace context and a flat universe, (ii) no rigorous derivation in the more involved inhomogeneous context (taking into account lattice refinement) has been provided so far, (iii) even if a derivation were possible, the inflationary energy scale would be too low for volume/curvature corrections to be sizable, and (iv) even setting aside the issue of their size, the analysis would remain incomplete because we do not know how these corrections compete with holonomy modifications of the dynamics. As an example for the claimed incompleteness of correction functions used, the independence of inverse-volume corrections of the connection or curvature has been criticized as physically unjustified.

We had already partially answered some of these objections elsewhere [8]. First, let us summarize the main arguments advanced there:

(i) In a realistic cosmological scenario, there is no conformal invariance of the scale factor and the correct way to implement the quantum dynamics is to consider the natural cell subdivision of space and how these cells evolve in time: this is the lattice refinement picture. In this perspective, interpretational difficulties regarding quantum corrections appear to be just an artifact of the idealized homogeneous and isotropic setting of pure minisuperspace models.

(ii) Although a rigorous derivation is desirable, the motivations of lattice refinement are natural in the perspective of the full quantum theory and there is no conceptual obstacle in relaxing the parametrization obtained in a pure minisuperspace.[4] Moreover, one cannot simply suppress inverse-volume corrections

---

[4]Sometimes, the argument is advanced that the minisuperspace parametrization (in particular, the so-called improved dynamics) is the only one producing a constant critical density and a robust bounce picture. This argument is invalid for two reasons. On one hand, even the improved dynamics

by a regularization procedure, as occasionally suggested by taking the limit of $\mathcal{V}_0 \to \infty$ in cases where these corrections are $\mathcal{V}_0$-dependent. Inverse-volume corrections do appear in the full quantum theory and play an important role for well-defined Hamiltonians. If they disappeared by a regularization procedure in minisuperspace models, one should explain why they are absent in a cosmological setting but not otherwise. Furthermore, there is tension between the requirement of closure of the inhomogeneous constraint algebra and the minisuperspace parametrization [8], which demands clarifications; although the lattice parametrization is so far implemented semi-heuristically in calculations of effective constraint algebras, it does accommodate anomaly cancellation.

(iii) Since the gauge symmetry of the model is deformed by quantum corrections, the very structure of spacetime is modified locally but everywhere; thus, one expects effects larger than in traditional scenarios of standard general relativity with higher-order curvature terms. In [8] we found qualitative theoretical estimates of these effects which are several orders of magnitude larger than minisuperspace estimates (and, interestingly, rather close to experimental bounds [9] in terms of orders of magnitude). However, the lack of control over the putative quantum gravity characteristic scale (hidden in the quantum corrections) makes it difficult to assess its importance within inflation.

(iv) We argued that other quantum corrections would not cancel inverse-volume effect because of the radically different way in which they affect the dynamics. Of course, the issue of comparing inverse-volume and holonomy corrections remains of interest for the community, but one does not expect that miraculous cancellations happen between the two.

The results of the present section serve to further address the above objections and provide final clarifications for several of them. For the first time, we have embedded inverse-volume corrections in inhomogeneous models, using the lattice refinement picture and working at the kinematical level, thus giving fresh insight to these issues. In particular:

(i)-(ii) When the phase space volume is associated with an individual homogeneous cell rather than a fiducial volume (as done in pure minisuperspace), the lattice parametrization emerges naturally and a quantum-gravity scale replaces unphysical quantities in inverse-volume corrections. Correction functions are completely independent of comoving volumes such as $\mathcal{V}_0$ and there is no regularization needed to make them disappear.

---

parametrization does *not* give a constant critical density unless quantization ambiguities are tuned to certain specific values [7]; the time-dependent modification comes from inverse-volume corrections in the gravitational sector, which are nonzero in general. On the other hand, within the lattice parametrization a constant critical density, if desired, can be obtained, indeed.

(iii) Surprisingly, the magnitude of these corrections can be argued to be large at mesoscopic scales, even when densities are far away from Planckian values such as during inflation. In cosmological models, quantum corrections are relevant not just near a bounce at Planckian density.

(iv) The basic noncancellation between inverse-volume effects and other, presently uncontrolled quantum corrections is reiterated with novel arguments. Modifications of the classical constraint algebra by inverse-volume corrections cannot cancel with those from holonomy corrections, nor with terms from quantum back-reaction. Holonomy corrections provide an additional connection dependence of almost-periodic type in the constraints, while inverse-volume corrections as shown here have only weak connection dependence. Inverse-triad corrections are also independent of moments of a state, as they would determine quantum back-reaction. The structure of the Poisson algebra on the quantum phase space, including expectation values and moments, shows that neither the connection-dependent terms of the form of holonomy corrections nor moment terms describing quantum back-reaction can cancel the terms of inverse-volume corrections. If the constraint algebra is modified by inverse-volume corrections, it must remain modified when all corrections are included. Thus, also the presence of effects larger than usually expected in quantum gravity is general.

To summarize, loop quantum cosmology implies the presence of inverse-volume corrections in its cosmological perturbation equations. In their general parametrization, the corrections depend only on triad variables simply because they depend on a quantum scale whose *dynamical* nature is encoded by the background scale factor. This conclusion is a result of the derivations presented here, not an assumption. Also, their power-law form as a function of the scale factor is suggested by very general semiclassical considerations which do not further restrict the class of states.

3. Inflationary observables

With a consistent implementation of inverse-volume corrections at hand, a complete set of cosmological perturbation equations follows. These equations have been derived elsewhere [1]-[5], starting with a constraint analysis. Here we continue to prepare these equations for a convenient cosmological investigation, which we then exploit to find observational bounds on some parameters.

3.1 Hubble slow-roll tower

The slow-roll parameters as functions of the Hubble rate are defined starting from the background equations of motion, which also determine the coefficients of the linear perturbation equations. In the presence of inverse-volume corrections, the effective

Friedmann and Klein–Gordon equations read

$$\mathcal{H}^2 = \frac{\kappa^2}{3}\,\alpha\left[\frac{\varphi'^2}{2\nu} + pV(\varphi)\right] \tag{3.1}$$

and

$$\varphi'' + 2\mathcal{H}\left(1 - \frac{\mathrm{d}\ln\nu}{\mathrm{d}\ln p}\right)\varphi' + \nu pV_{,\varphi} = 0\,, \tag{3.2}$$

respectively, where primes denote derivatives with respect to conformal time $\tau := \int \mathrm{d}t/a$, $\mathcal{H} := a'/a = aH$, $\kappa^2 = 8\pi G$, G is Newton's constant, and φ is a real scalar field with potential $V(\varphi)$. Following section 2, the LQC correction functions are of the form

$$\alpha = 1 + \alpha_0\delta_{\mathrm{Pl}}, \tag{3.3}$$

$$\nu = 1 + \nu_0\delta_{\mathrm{Pl}}, \tag{3.4}$$

where α_0 and ν_0 are constants and

$$\delta_{\mathrm{Pl}} \propto a^{-\sigma} \tag{3.5}$$

is a quantum correction (2.16) whose time dependence is modelled as a power of the scale factor (here $\sigma > 0$ is another constant). The proportionality factor will never enter the analysis explicitly but, in the derivation of the perturbation equations, it is assumed that $\delta_{\mathrm{Pl}} < 1$. Consistently, throughout the paper we use the equality symbol = for expressions valid up to $O(\delta_{\mathrm{Pl}})$ terms, while we employ $\approx$ for relations where the slow-roll approximation has been used. The latter holds when the following slow-roll parameters are small:

$$\epsilon := 1 - \frac{\mathcal{H}'}{\mathcal{H}^2}$$
$$= \frac{\kappa^2}{2}\frac{\varphi'^2}{\mathcal{H}^2}\left\{1 + \left[\alpha_0 + \nu_0\left(\frac{\sigma}{6} - 1\right)\right]\delta_{\mathrm{Pl}}\right\} + \frac{\sigma\alpha_0}{2}\delta_{\mathrm{Pl}}\,, \tag{3.6}$$

$$\eta := 1 - \frac{\varphi''}{\mathcal{H}\varphi'}\,. \tag{3.7}$$

The conformal-time derivatives of ϵ and η are

$$\epsilon' = 2\mathcal{H}\epsilon(\epsilon - \eta) - \sigma\mathcal{H}\tilde{\epsilon}\delta_{\mathrm{Pl}}\,, \tag{3.8}$$

$$\eta' = \mathcal{H}(\epsilon\eta - \xi^2)\,, \tag{3.9}$$

where

$$\tilde{\epsilon} := \alpha_0\left(\frac{\sigma}{2} + 2\epsilon - \eta\right) + \nu_0\left(\frac{\sigma}{6} - 1\right)\epsilon\,. \tag{3.10}$$

The inflationary spectra were computed in [8]. The scalar power spectrum is

$$\mathcal{P}_{\mathrm{s}} = \frac{G\mathcal{H}^2}{\pi a^2\epsilon}(1 + \gamma_{\mathrm{s}}\delta_{\mathrm{Pl}})\,, \tag{3.11}$$

where

$$\gamma_{\rm s} := \nu_0 \left(\frac{\sigma}{6} + 1\right) + \frac{\sigma \alpha_0}{2\epsilon} - \frac{\chi}{\sigma + 1}, \qquad \chi := \frac{\sigma \nu_0}{3}\left(\frac{\sigma}{6} + 1\right) + \frac{\alpha_0}{2}\left(5 - \frac{\sigma}{3}\right). \qquad (3.12)$$

Equation (3.11) is evaluated at the time $k = \mathcal{H}$ when the perturbation with comoving wavenumber k crosses the Hubble horizon. Using the fact that

$$\delta'_{\rm Pl} = -\sigma \mathcal{H} \delta_{\rm Pl} \qquad (3.13)$$

and $' \approx \mathcal{H} \, d/d \ln k$, the scalar spectral index $n_{\rm s} - 1 := d \ln \mathcal{P}_{\rm s}/d \ln k$ reads

$$n_{\rm s} - 1 = 2\eta - 4\epsilon + \sigma \gamma_{n_{\rm s}} \delta_{\rm Pl}, \qquad (3.14)$$

where

$$\gamma_{n_{\rm s}} := \frac{\tilde{\epsilon}}{\epsilon} - \alpha_0 \left(1 - \frac{\eta}{\epsilon}\right) - \gamma_{\rm s} = \alpha_0 - 2\nu_0 + \frac{\chi}{\sigma + 1}, \qquad (3.15)$$

while the running $\alpha_{\rm s} := dn_{\rm s}/d \ln k$ is

$$\alpha_{\rm s} = 2(5\epsilon\eta - 4\epsilon^2 - \xi^2) + \sigma(4\tilde{\epsilon} - \sigma \gamma_{n_{\rm s}})\delta_{\rm Pl}. \qquad (3.16)$$

This shows that, for $\sigma = O(1)$, the running can be as large as $\delta_{\rm Pl}$. In this case, the terms higher than the running can give rise to the contribution of the order of $\delta_{\rm Pl}$. In section 4.1 we shall address this issue properly.

The tensor power spectrum is

$$\mathcal{P}_{\rm t} = \frac{16G\mathcal{H}^2}{\pi a^2}(1 + \gamma_{\rm t}\delta_{\rm Pl}), \qquad \gamma_{\rm t} = \frac{\sigma - 1}{\sigma + 1}\alpha_0, \qquad (3.17)$$

while its index $n_{\rm t} := d \ln \mathcal{P}_{\rm t}/d \ln k$ and running $\alpha_{\rm t} := dn_{\rm t}/d \ln k$ are, respectively,

$$n_{\rm t} = -2\epsilon - \sigma \gamma_{\rm t}\delta_{\rm Pl}, \qquad (3.18)$$

and

$$\alpha_{\rm t} = -4\epsilon(\epsilon - \eta) + \sigma(2\tilde{\epsilon} + \sigma \gamma_{\rm t})\delta_{\rm Pl}. \qquad (3.19)$$

The tensor-to-scalar ratio $r := \mathcal{P}_{\rm t}/\mathcal{P}_{\rm s}$ combines with the tensor index into a consistency relation:

$$\begin{aligned} r &= 16\epsilon\left[1 + (\gamma_{\rm t} - \gamma_{\rm s})\delta_{\rm Pl}\right] \\ &= -8\{n_{\rm t} + [n_{\rm t}(\gamma_{\rm t} - \gamma_{\rm s}) + \sigma\gamma_{\rm t}]\delta_{\rm Pl}\}. \end{aligned} \qquad (3.20)$$

When $\delta_{\rm Pl} = 0$, all the above formulas agree with the standard classical scenario [27].

3.2 Potential slow-roll tower

To constrain the inflationary potential against observations, it is convenient to recast the cosmological observables in terms of the tower of slow-roll parameters written as functions of V and its derivatives. From Eqs. (3.1) and (3.6) we have

$$\frac{\kappa^2}{2}\frac{\varphi'^2}{\mathcal{H}^2} = \epsilon - \left\{\frac{\sigma\alpha_0}{2} + \epsilon\left[\alpha_0 + \nu_0\left(\frac{\sigma}{6}-1\right)\right]\right\}\delta_{\text{Pl}}\,, \tag{3.21}$$

$$\nu p V = \left(3\frac{\nu}{\alpha} - \frac{\kappa^2}{2}\frac{\varphi'^2}{\mathcal{H}^2}\right)\frac{\mathcal{H}^2}{\kappa^2}$$

$$= \frac{3\mathcal{H}^2}{\kappa^2}\left(1 - \frac{\epsilon}{3} + \left\{\nu_0 + \alpha_0\left(\frac{\sigma}{6}-1\right) + \frac{\epsilon}{3}\left[\alpha_0 + \nu_0\left(\frac{\sigma}{6}-1\right)\right]\right\}\delta_{\text{Pl}}\right), \tag{3.22}$$

$$V_{,\varphi} = -\frac{3\mathcal{H}\varphi'}{\nu p}\left(1 - \frac{\eta}{3} + \frac{\sigma\nu_0}{3}\delta_{\text{Pl}}\right)\,, \tag{3.23}$$

$$V_{,\varphi\varphi} = \frac{\mathcal{H}^2}{\nu p}\left[3(\epsilon+\eta) - \eta^2 - \xi^2 - (3-\sigma-\epsilon-2\eta)\sigma\nu_0\delta_{\text{Pl}}\right]\,, \tag{3.24}$$

$$V_{,\varphi\varphi\varphi} = -\frac{3\mathcal{H}^3}{\nu p\varphi'}\left(\xi^2 + 3\epsilon\eta - \sigma\left\{\nu_0\left[\left(1-\frac{2\sigma}{3}\right)\eta + (3-\sigma)\left(\epsilon+\frac{\sigma}{3}\right)\right.\right.\right.$$
$$\left.\left.\left. - \frac{4}{3}\epsilon\eta - \frac{1}{3}\eta^2 - \xi^2\right] - \tilde{\epsilon}\right\}\delta_{\text{Pl}}\right)\,. \tag{3.25}$$

The first three elements of the tower are

$$\epsilon_V := \frac{1}{2\kappa^2}\left(\frac{V_{,\varphi}}{V}\right)^2\,, \qquad \eta_V := \frac{1}{\kappa^2}\frac{V_{,\varphi\varphi}}{V}\,, \qquad \xi_V^2 := \frac{V_{,\varphi}V_{,\varphi\varphi\varphi}}{\kappa^4 V^2}\,. \tag{3.26}$$

On using Eqs. (3.23)–(3.25), we have the following technical expressions:

$$\epsilon_V \approx \epsilon + \left\{-\frac{\sigma\alpha_0}{2} + \frac{\sigma\alpha_0}{3}\eta + \left[\alpha_0\left(1-\frac{2\sigma}{3}\right) + \nu_0\left(\frac{\sigma}{2}-1\right)\right]\epsilon\right\}\delta_{\text{Pl}}\,, \tag{3.27a}$$

$$\eta_V \approx \epsilon + \eta + \left\{\sigma\nu_0\left(\frac{\sigma}{3}-1\right) + \left[\alpha_0\left(1-\frac{\sigma}{6}\right) + \nu_0\left(\frac{2\sigma}{3}-1\right)\right]\eta\right.$$
$$\left. + \left[\alpha_0\left(1-\frac{\sigma}{6}\right) + \nu_0\left(\frac{\sigma^2}{9}-1\right)\right]\epsilon\right\}\delta_{\text{Pl}}\,, \tag{3.27b}$$

$$\xi_V^2 \approx \xi^2 + 3\epsilon\eta + \left[\sigma f_\xi(\epsilon,\eta) + g_\xi(\epsilon,\eta,\xi^2)\right]\delta_{\text{Pl}}\,, \tag{3.27c}$$

$$f_\xi(\epsilon,\eta) := \sigma\left[\frac{\alpha_0}{2} + \nu_0\left(\frac{\sigma}{3}-1\right)\right] + \left[2\alpha_0\left(\frac{\sigma}{6}+1\right) - \nu_0\left(4-\frac{\sigma}{2}-\frac{2\sigma^2}{9}\right)\right]\epsilon$$
$$- \left[\alpha_0\left(\frac{\sigma}{6}+1\right) + \nu_0\left(1-\sigma+\frac{\sigma^2}{9}\right)\right]\eta\,,$$

$$g_\xi(\epsilon,\eta,\xi^2) := \left[\alpha_0\left(4+\frac{\sigma}{2}\right) - \nu_0\left(8-\frac{4\sigma}{3}-\frac{\sigma^2}{3}\right)\right]\frac{\sigma}{3}\epsilon^2 + \left[\alpha_0 + 2\nu_0\left(1-\frac{\sigma}{3}\right)\right]\frac{\sigma}{3}\eta^2$$
$$+ \left[\alpha_0\left(6-\frac{7\sigma}{3}-\frac{\sigma^2}{9}\right) - \nu_0\left(6-3\sigma-\frac{5\sigma^2}{18}+\frac{2\sigma^3}{27}\right)\right]\epsilon\eta$$
$$+ 2\left[\alpha_0\left(1-\frac{\sigma}{6}\right) + \nu_0\left(\frac{2\sigma}{3}-1\right)\right]\xi^2\,, \tag{3.27d}$$

which give the inversion formulas

$$\epsilon \approx \epsilon_V + \left\{ \frac{\sigma \alpha_0}{2} - \left[\alpha_0 \left(1 - \sigma \right) + \nu_0 \left(\frac{\sigma}{2} - 1 \right) \right] \epsilon_V - \frac{\sigma \alpha_0}{3} \eta_V \right\} \delta_{\text{Pl}} , \qquad (3.28a)$$

$$\eta \approx \eta_V - \epsilon_V$$
$$- \left\{ \sigma \left(\frac{\alpha_0}{2} + \frac{\sigma \nu_0}{3} - \nu_0 \right) + \left[\alpha_0 \left(\sigma - 1 \right) + \nu_0 \left(1 - \frac{7\sigma}{6} + \frac{\sigma^2}{9} \right) \right] \epsilon_V$$
$$+ \left[\alpha_0 \left(1 - \frac{\sigma}{2} \right) + \nu_0 \left(\frac{2\sigma}{3} - 1 \right) \right] \eta_V \right\} \delta_{\text{Pl}} , \qquad (3.28b)$$

$$\xi^2 \approx \xi_V^2 + 3\epsilon_V^2 - 3\epsilon_V \eta_V$$
$$+ \left\{ \sigma^2 \left[\nu_0 \left(1 - \frac{\sigma}{3} \right) - \frac{\alpha_0}{2} \right] + \sigma^2 \left[-\frac{\alpha_0}{2} + \nu_0 \left(\frac{3}{2} - \frac{\sigma}{3} \right) \right] \epsilon_V$$
$$+ \sigma \left[\frac{\alpha_0}{2} \left(\frac{\sigma}{3} - 1 \right) + \nu_0 \left(1 - \sigma + \frac{\sigma^2}{9} \right) \right] \eta_V + \frac{2}{3} \left[\alpha_0 + \nu_0 \left(\frac{\sigma}{3} - 1 \right) \right] \sigma \eta_V^2$$
$$+ \left[-\alpha_0 \left(6 - 3\sigma + \frac{5\sigma^2}{18} \right) + \nu_0 \left(6 - 4\sigma + \frac{7\sigma^2}{18} - \frac{5\sigma^3}{27} \right) \right] \epsilon_V^2$$
$$+ \left[\alpha_0 \left(6 - \frac{7\sigma}{2} + \frac{\sigma^2}{9} \right) - \nu_0 \left(6 - \frac{35\sigma}{6} + \frac{13\sigma^2}{18} - \frac{2\sigma^3}{27} \right) \right] \epsilon_V \eta_V$$
$$+ \left[\alpha_0 \left(\frac{\sigma}{3} - 2 \right) + 2\nu_0 \left(1 - \frac{2\sigma}{3} \right) \right] \xi_V^2 \right\} \delta_{\text{Pl}} . \qquad (3.28c)$$

We can now rewrite the cosmological observables. The scalar index (3.14) and its running (3.16) become

$$n_{\text{s}} - 1 = -6\epsilon_V + 2\eta_V - c_{n_{\text{s}}} \delta_{\text{Pl}} , \qquad (3.29)$$

$$\alpha_{\text{s}} = -24\epsilon_V^2 + 16\epsilon_V \eta_V - 2\xi_V^2 + c_{\alpha_{\text{s}}} \delta_{\text{Pl}} , \qquad (3.30)$$

where

$$c_{n_{\text{s}}} = f_{\text{s}} - \left[6\alpha_0 \left(1 - \sigma \right) - \nu_0 \left(6 - \frac{13\sigma}{3} + \frac{2\sigma^2}{9} \right) \right] \epsilon_V$$
$$- \left[\alpha_0 \left(\frac{7\sigma}{3} - 2 \right) + 2\nu_0 \left(1 - \frac{2\sigma}{3} \right) \right] \eta_V , \qquad (3.31a)$$

$$c_{\alpha_s} = \sigma f_s + \left[\alpha_0\sigma(\sigma-6) + \nu_0\sigma\left(6 - \frac{17\sigma}{3} + \frac{2\sigma^2}{3}\right)\right]\epsilon_V$$

$$+ \left[\alpha_0\sigma\left(2 - \frac{\sigma}{3}\right) - 2\nu_0\sigma\left(1 - \sigma + \frac{\sigma^2}{9}\right)\right]\eta_V$$

$$+ \left[\alpha_0\left(48 - 42\sigma + \frac{5\sigma^2}{9}\right) - \nu_0\left(48 - \frac{98\sigma}{3} + \frac{17\sigma^2}{9} - \frac{10\sigma^3}{27}\right)\right]\epsilon_V^2$$

$$+ \left[-\frac{14\sigma\alpha_0}{3} + \frac{4\sigma\nu_0}{3}\left(1 - \frac{\sigma}{3}\right)\right]\eta_V^2$$

$$+ \left[2\alpha_0\left(-16 + \frac{46\sigma}{3} - \frac{\sigma^2}{9}\right) + \nu_0\left(32 - \frac{70\sigma}{3} + \frac{13\sigma^2}{9} - \frac{4\sigma^3}{27}\right)\right]\epsilon_V\eta_V$$

$$+ \left[2\alpha_0\left(2 - \frac{\sigma}{3}\right) + 4\nu_0\left(\frac{2\sigma}{3} - 1\right)\right]\xi_V^2, \tag{3.31b}$$

$$f_s := \frac{\sigma[3\alpha_0(13\sigma - 3) + \nu_0\sigma(6 + 11\sigma)]}{18(\sigma + 1)}. \tag{3.31c}$$

The tensor index (3.18) and its running (3.19) are

$$n_t = -2\epsilon_V - c_{n_t}\delta_{\text{Pl}}, \tag{3.32}$$

$$\alpha_t = -4\epsilon_V(2\epsilon_V - \eta_V) + c_{\alpha_t}\delta_{\text{Pl}}, \tag{3.33}$$

where

$$c_{n_t} = f_t - [2\alpha_0(1 - \sigma) + \nu_0(\sigma - 2)]\epsilon_V - \frac{2\sigma\alpha_0}{3}\eta_V, \tag{3.34}$$

$$c_{\alpha_t} = \sigma f_t + \sigma[(2 - \sigma)\nu_0 - 2\alpha_0]\epsilon_V + \left[16\alpha_0(1 - \sigma) - 4\nu_0\left(4 - \frac{8\sigma}{3} + \frac{\sigma^2}{9}\right)\right]\epsilon_V^2$$

$$- \frac{4\sigma\alpha_0}{3}\eta_V^2 + \left[2\alpha_0(5\sigma - 4) + 2\nu_0\left(4 - \frac{7\sigma}{3}\right)\right]\epsilon_V\eta_V, \tag{3.35}$$

$$f_t := \frac{2\sigma^2\alpha_0}{\sigma + 1}. \tag{3.36}$$

Finally, the tensor-to-scalar ratio (3.20) is

$$r = 16\epsilon_V + c_r\delta_{\text{Pl}}, \tag{3.37}$$

where

$$c_r = \frac{8[3\alpha_0(3 + 5\sigma + 6\sigma^2) - \nu_0\sigma(6 + 11\sigma)]}{9(\sigma + 1)}\epsilon_V - \frac{16\sigma\alpha_0}{3}\eta_V. \tag{3.38}$$

4. Power spectra and cosmic variance

In this section, we cast the power spectra as nonperturbative functions of the wavenumber k and a pivot scale k_0 (section 4.1). The parameter space of the numerical analysis is introduced in section 4.2, while a theoretical prior on the size of the quantum correction is discussed in section 4.3. An important question to address is whether a

possible LQC signal at large scales would be stronger than cosmic variance, which is the dominant effect at low multipoles. This issue is considered in section 4.4, where a positive answer is given for a certain range in the parameter space.

4.1 Power spectra and pivot scales

Because of Eq. (3.13), terms higher than the runnings $\alpha_{\rm s}$ and $\alpha_{\rm t}$ can give rise to a nonnegligible contribution to the power spectra $\mathcal{P}_{\rm s}(k)$ and $\mathcal{P}_{\rm t}(k)$. Let us expand the scalar power spectrum to all orders in the perturbation wavenumber about a pivot scale k_0:

$$\ln \mathcal{P}_{\rm s}(k) = \ln \mathcal{P}_{\rm s}(k_0) + [n_{\rm s}(k_0) - 1]x + \frac{\alpha_{\rm s}(k_0)}{2}x^2 + \sum_{m=3}^{\infty} \frac{\alpha_{\rm s}^{(m)}(k_0)}{m!}x^m \,, \tag{4.1}$$

where $x := \ln(k/k_0)$, and $\alpha_{\rm s}^{(m)} := {\rm d}^{m-2}\alpha_{\rm s}/({\rm d}\ln k)^{m-2}$. When $O(\epsilon_V)$ and $O(\eta_V)$ terms are ignored, $c_{n_{\rm s}} \approx f_{\rm s}$ in Eq. (3.29), while the dominant contribution to the scalar running can be estimated as

$$\alpha_{\rm s}(k_0) = \left.\frac{{\rm d}n_{\rm s}}{{\rm d}\ln k}\right|_{k=k_0} \approx \sigma f_{\rm s}\delta_{\rm Pl}(k_0) \,. \tag{4.2}$$

Similarly, we can derive the m-th order terms $\alpha_{\rm s}^{(m)}$ as

$$\alpha_{\rm s}^{(m)}(k_0) \approx (-1)^m \sigma^{m-1} f_{\rm s}\delta_{\rm Pl}(k_0) \,. \tag{4.3}$$

In this case, the last term in Eq. (4.1) converges to the exponential series,

$$\sum_{m=3}^{\infty} \frac{\alpha_{\rm s}^{(m)}(k_0)}{m!}x^m = f_{\rm s}\delta_{\rm Pl}(k_0) \left[x\left(1 - \frac{1}{2}\sigma x\right) + \frac{1}{\sigma}(e^{-\sigma x} - 1)\right] \,. \tag{4.4}$$

Thus, the scalar power spectrum (4.1) can be written in the form

$$\mathcal{P}_{\rm s}(k) = \mathcal{P}_{\rm s}(k_0) \exp\left\{[n_{\rm s}(k_0) - 1]x + \frac{\alpha_{\rm s}(k_0)}{2}x^2 \right.$$
$$\left. + f_{\rm s}\delta_{\rm Pl}(k_0)\left[x\left(1 - \frac{1}{2}\sigma x\right) + \frac{1}{\sigma}(e^{-\sigma x} - 1)\right]\right\} \,. \tag{4.5}$$

This expression is valid for any value of σ and of the pivot wavenumber, provided the latter lies within the observational range of the experiment. Note that k_0 is not fixed observationally and we can choose any value on the scales relevant to CMB (with the multipoles ℓ ranging in the region $2 < \ell < 1000$). The CMB multipoles are related to the wavenumber k by the approximate relation

$$k \approx 10^{-4} h\,\ell \ \ {\rm Mpc}^{-1} \,, \tag{4.6}$$

where we take the value $h = 0.7$ for the reduced Hubble constant. The default pivot value of CMBFAST [28] and CAMB [29] codes is $k_0 = 0.05$ Mpc^{-1} ($\ell_0 \sim 730$). For the WMAP pivot scale $k_0 = 0.002$ Mpc^{-1} ($\ell \sim 29$) [30, 31], the maximum value of x relevant to the CMB anisotropies is $x_{\max} \sim 3.6$. Intermediate values of k_0 are also possible, for instance $k_0 = 0.01$ Mpc^{-1} [32]. In general, the constraints on the parameter space, and in particular the likelihood contours, depend (even strongly) on the choice of the pivot scale [33], and it is interesting to compare results with different k_0 also in LQC.

The fact that we can resum the whole series is of utmost importance for the consistency of the numerical analysis. In standard inflation, higher-order terms do not contribute to the power spectrum because they are higher-order in the slow-roll parameters. Then, one can truncate Eq. (4.1) to the first three terms and ignore the others. Here, on the other hand, all the terms (4.3) are linear in $\delta_{\rm Pl}$ and they contribute equally if the parameter σ is large enough, $\sigma \gtrsim 1$. This fact might naively suggest that small values of σ are preferred for a consistent analysis of a quasi-scale-invariant spectrum [8]. In that case, one would have to impose conditions such as $|[n_{\rm s}(k_0) - 1]x| \gg |[\alpha_{\rm s}(k_0)/2]x^2|$, which depend on the pivot scale k_0.

For $\sigma > 1$, however, different choices of k_0 would result in different convergence properties of the Taylor expansion of $\mathcal{P}_{\rm s}$. The point is that $\delta_{\rm Pl}(k)$ changes fast for $\sigma > 1$ and the running of the spectral index can be sizable; dropping higher-order terms would eventually lead to inconsistent results. On the other hand, Eq. (4.5) does not suffer from any of the above limitations and problems, and it will be the basis of our analysis, where $n_{\rm s}(k_0)$ and $\alpha_{\rm s}(k_0)$ are given by Eqs. (3.31a) and (3.31a). The last term in Eq. (4.5), usually negative, tends to compensate the large positive running, thus providing a natural scale-invariance mechanism without putting any numerical priors.

Assuming that $c_{n_{\rm t}} \approx f_{\rm t}$, same considerations hold for the tensor spectrum, which can be written as

$$
\mathcal{P}_{\rm t}(k) = \mathcal{P}_{\rm t}(k_0) \exp \left\{ n_{\rm t}(k_0)\, x + \frac{\alpha_{\rm t}(k_0)}{2} x^2 \right.
$$
$$
\left. + f_{\rm t}\delta_{\rm Pl}(k_0) \left[x \left(1 - \frac{1}{2}\sigma x \right) + \frac{1}{\sigma}(e^{-\sigma x} - 1) \right] \right\},
\tag{4.7}
$$

where $n_{\rm t}(k_0)$ and $\alpha_{\rm t}(k_0)$ are given by Eqs. (3.32) and (3.33), respectively. Finally, the tensor-to-scalar ratio is given by Eqs. (3.37) and (3.38), with the slow-roll parameters evaluated at the pivot scale $k = k_0$.

4.2 Parameter space

The CMB likelihood analysis can be carried out by using Eqs. (4.5), (4.7), and (3.37). Let us take the power-law potential [34]

$$
V(\varphi) = V_0 \varphi^n .
\tag{4.8}
$$

In this case, it follows that (k_0 dependence implicit)

$$\epsilon_V = \frac{n^2}{2\kappa^2\varphi^2}, \qquad \eta_V = \frac{2(n-1)}{n}\epsilon_V, \qquad \xi_V^2 = \frac{4(n-1)(n-2)}{n^2}\epsilon_V^2. \qquad (4.9)$$

This allows us to reduce the slow-roll parameters to one (i.e., ϵ_V).

For the exponential potential [35]

$$V(\varphi) = V_0 e^{-\kappa\lambda\varphi}, \qquad (4.10)$$

the relation between the slow-roll parameters is given by

$$\epsilon_V = \frac{\lambda^2}{2}, \qquad \eta_V = 2\epsilon_V, \qquad \xi_V^2 = 4\epsilon_V^2, \qquad (4.11)$$

which are again written in terms of the single parameter ϵ_V.

Between the model parameters ν_0 and α_0 we can also impose the following relation [8], valid for $\sigma \neq 3$:

$$\nu_0 = \frac{3(\sigma-6)}{(\sigma+6)(\sigma-3)}\alpha_0. \qquad (4.12)$$

Introducing the variable

$$\delta(k_0) := \alpha_0\delta_{\mathrm{Pl}}(k_0), \qquad (4.13)$$

we can write $f_s\delta_{\mathrm{Pl}}(k_0)$ and $f_t\delta_{\mathrm{Pl}}(k_0)$ in the form

$$f_s\delta_{\mathrm{Pl}}(k_0) = \frac{\sigma(8\sigma^3 - 8\sigma^2 - 93\sigma + 18)}{2(\sigma-3)(\sigma+1)(\sigma+6)}\delta(k_0), \qquad f_t\delta_{\mathrm{Pl}}(k_0) = \frac{2\sigma^2}{\sigma+1}\delta(k_0). \qquad (4.14)$$

For $\sigma = 3$ one has $\alpha_0 = 0$ identically, in which case Eq. (4.13) is replaced by $\delta(k_0) := \nu_0\delta_{\mathrm{Pl}}(k_0)$.

To summarize, using the relation (4.12), all the other observables can be written in terms of $\delta(k_0)$ and $\epsilon_V(k_0)$. Hence, for given σ and k_0, one can perform the CMB likelihood analysis by varying the two parameters $\delta(k_0)$ and $\epsilon_V(k_0)$.

4.3 Theoretical upper bound on the quantum correction

For the validity of the linear expansion of the correction functions (3.3) and (3.4)[5] and all the perturbation formulas where the $O(\delta_{\mathrm{Pl}})$ truncation has been systematically implemented, we require that $\delta(k) = \alpha_0\delta_{\mathrm{Pl}}(k) < 1$ for all wavenumbers relevant to the CMB anisotropies. Since $\delta_{\mathrm{Pl}} \propto a^{-\sigma}$, the quantity $\delta(k)$ appearing in inflationary observables is approximately given by

$$\delta(k) = \delta(k_0)\left(\frac{k_0}{k}\right)^\sigma, \qquad (4.15)$$

---

[5]Using the relation (4.12), one sees that ν_0 is of the same order as α_0, so a bound on δ is sufficient.

where we have used $k = \mathcal{H}$ at Hubble exit with $\mathcal{H}/a \approx$ const. As $k \propto \ell$, the same expression can be written in terms of the multipoles ℓ. Since $\sigma > 0$, one has $\delta(k) > \delta(k_0)$ for $k < k_0$ and $\delta(k) < \delta(k_0)$ for $k > k_0$. This means that the larger the pivot scale k_0, the smaller the upper bound on $\delta(k_0)$.

Let us consider two pivot scales: (i) $k_0 = 0.002$ Mpc^{-1} (multipole $\ell_0 \sim 29$) and (ii) $k_0 = 0.05$ Mpc^{-1} (multipole $\ell_0 \sim 730$). Since the largest scale in CMB corresponds to the quadrupole $\ell = 2$, the condition $\delta(k) < 1$ at $\ell = 2$ gives the following bounds δ_{max} on the values of $\delta(k_0)$ with two pivot scales:

$$\text{(i)} \quad \delta_{\mathrm{max}} = 14.5^{-\sigma} \qquad \text{(for} \quad k_0 = 0.002 \text{ Mpc}^{-1}), \tag{4.16}$$

$$\text{(ii)} \quad \delta_{\mathrm{max}} = 365^{-\sigma} \qquad \text{(for} \quad k_0 = 0.05 \text{ Mpc}^{-1}). \tag{4.17}$$

Values of δ_{max} for some choices of σ are reported in table 1. The suppression of δ_{max} for larger k_0 and σ can be also seen in the power spectra (4.5) and (4.7). The term $e^{-\sigma x} = (k_0/k)^\sigma$ can be very large for large k_0: for instance, if $\sigma = 6$ and $k_0 = 0.05$ Mpc^{-1}, one has $e^{-\sigma x} \sim 10^{15}$ at $\ell = 2$. Then we require that $\delta(k_0)$ is suppressed as $\delta(k_0) \lesssim 10^{-16}$.

σ	0.5	1	1.5	2	3	6
$k_0 = 0.002$ Mpc^{-1}						
δ_{max}	0.26	6.9×10^{-2}	1.8×10^{-2}	4.7×10^{-3}	3.2×10^{-4}	1.0×10^{-7}
δ	0.27	3.5×10^{-2}	1.7×10^{-3}	6.8×10^{-5}	4.3×10^{-7}	–
$k_0 = 0.05$ Mpc^{-1}						
δ_{max}	5.2×10^{-2}	2.7×10^{-3}	1.4×10^{-4}	7.5×10^{-6}	2.1×10^{-8}	4.3×10^{-16}
δ	6.7×10^{-2}	9.0×10^{-4}	1.3×10^{-5}	1.2×10^{-7}	2.7×10^{-11}	–

Table 1: Theoretical priors on the upper bound of δ ($= \delta_{\mathrm{max}}$) and 95% CL upper limits of δ constrained by observations for the potential $V(\varphi) = V_0 \varphi^2$ with different values of σ and for two pivot scales. The likelihood analysis has not been performed for $\sigma = 6$ since the signal is below the cosmic variance threshold already when $\sigma = 2$. For $\sigma = 3$, the parameter $\delta = \nu_0 \delta_{\mathrm{Pl}}$ has been used.

4.4 Cosmic variance

At large scales, the failure of the ergodic theorem for the CMB multipole spectrum manifests itself in the phenomenon of cosmic variance, an intrinsic uncertainty on observations due to the small samples at low multipoles. For a power spectrum $\mathcal{P}(\ell)$, cosmic variance is given by [36]

$$\mathrm{Var}_{\mathcal{P}}(\ell) = \frac{2}{2\ell + 1} \mathcal{P}^2(\ell). \tag{4.18}$$

A natural question, which is often overlooked in the literature of exotic cosmologies, is how effects coming from new physics compete with cosmic variance. In our particular

case, we would like to find which values of σ give rise to a theoretical upper bound $\delta_{\max}$ of inverse-volume LQC quantum corrections larger than the error bars due to cosmic variance *with respect to the classical spectrum.*

Consider the scalar spectrum $\mathcal{P}_s(\ell)$, Eq. (4.5) with k/k_0 replaced by ℓ/ℓ_0. It is determined up to the normalization $\mathcal{P}_s(\ell_0)$, so that the region in the $(\ell, \mathcal{P}_s(\ell)/\mathcal{P}_s(\ell_0))$ plane affected by cosmic variance is roughly delimited by the two curves

$$\frac{\mathcal{P}_s(\ell) \pm \sqrt{\mathrm{Var}_{\mathcal{P}_s}(\ell)}}{\mathcal{P}_s(\ell_0)}\bigg|_{\delta_{\mathrm{Pl}}=0} = \left(1 \pm \sqrt{\frac{2}{2\ell+1}}\right)\frac{\mathcal{P}_s(\ell)}{\mathcal{P}_s(\ell_0)}\bigg|_{\delta_{\mathrm{Pl}}=0}, \tag{4.19}$$

where we take the classical spectrum as reference.

The power spectrum (4.5), together with the cosmic variance effect (4.19), is shown in figure 1 for $n = 2$ and the pivot scale $\ell_0 = 29$. Ignoring the solid lines for the moment, the dashed curves correspond to $\delta = \delta_{\max}$. The exponential term $e^{-\sigma x} = (k_0/k)^\sigma$ in Eq. (4.5) gives rise to an enhancement of the power spectra on large scales, as we see in the figures. For $\sigma \gtrsim 3$, the growth of this term is so significant that $\delta(\ell)$ must be very much smaller than 1 for most of the scales observed in the CMB, in order to satisfy the bound $\delta(\ell = 2) < 1$. LQC inverse-volume corrections are well within the cosmic variance region for $\sigma > 2$. However, already at $\sigma = 2$ quantum corrections strongly affect multipoles $\ell \leq 6$. For $\sigma \sim 1$, the spectrum is appreciably modified also at multipoles $\ell \gtrsim 500$. Changing the pivot scale to $\ell_0 = 730$, one sees that the quantum effect is generally greater than cosmic variance at sufficiently low multipoles (figure 2). The plots for $n = 4$ are very similar and we shall omit them.
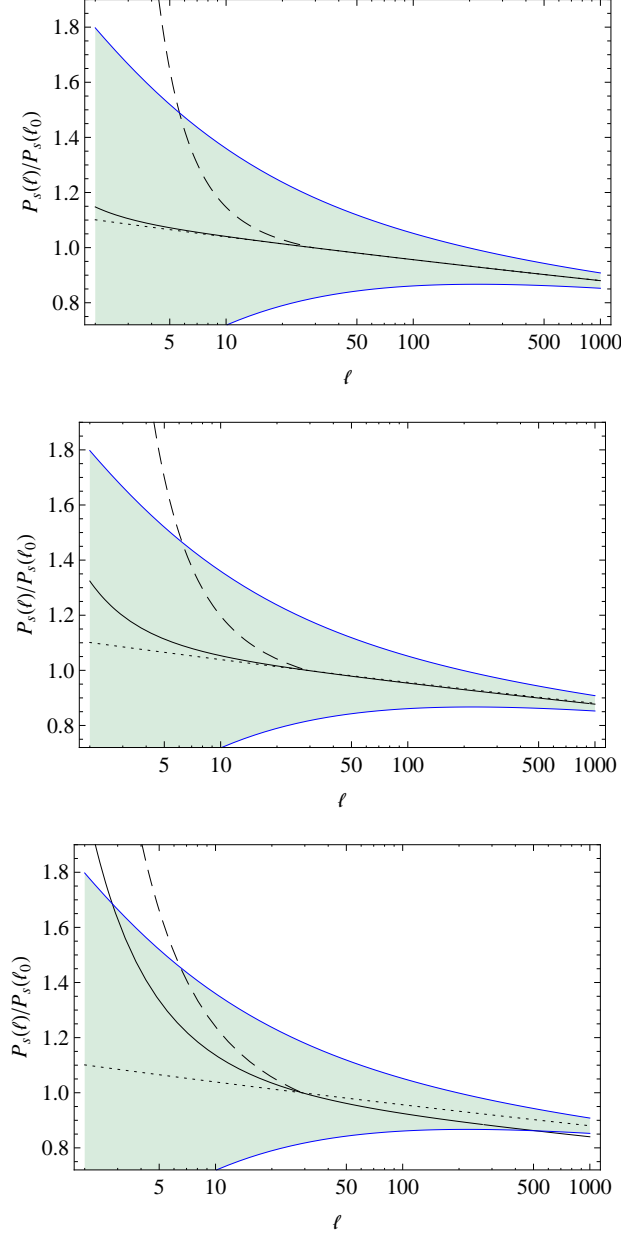
5. Likelihood analysis

We carry out the CMB likelihood analysis for the power-law potential (4.8) as well as the exponential potential (4.10). We run the Cosmological Monte Carlo (CosmoMC) code [29] with the data of WMAP 7yr [31] combined with large-scale structure (LSS) [37] (including BAO), HST [38], Supernovae type Ia (SN Ia) [39], and Big Bang Nucleosynthesis (BBN) [40], by assuming a ΛCDM model. Compared to our previous paper [9] in which the data of WMAP 7yr, BAO, and HST were used, we have included other observational data.

In the Monte Carlo routine we vary two inflationary parameters $\delta(k_0)$ and $\epsilon_V(k_0)$ as well as other cosmological parameters. Note that $\delta(k_0)$ and $\epsilon_V(k_0)$ are constrained at the chosen pivot scale k_0. While the bound on δ depends on k_0 (and it tends to be smaller for larger k_0), that on $(k_0)^\sigma \delta(k_0)$ does not [see Eq. (4.15)].

Under the conditions $\epsilon_V \ll 1$ and $\delta \ll 1$, the slow-roll parameter ϵ_V is approximately given by $\epsilon_V \approx (\kappa^2/2)(\varphi'/\mathcal{H})^2$. Then the number of e-foldings during inflation can be estimated as

$$N := \int_\tau^{\tau_{\mathrm{f}}} \mathrm{d}\tilde{\tau}\, \mathcal{H} \approx \kappa \int_{\varphi_{\mathrm{f}}}^\varphi \mathrm{d}\tilde{\varphi}\, \frac{1}{\sqrt{2\epsilon_V(\tilde{\varphi})}}, \tag{5.1}$$

Figure 1: Primordial scalar power spectrum $\mathcal{P}_{\mathrm{s}}(\ell)$ for the case $n = 2$, with $\epsilon_V(k_0) = 0.009$ and the pivot wavenumber $k_0 = 0.002\,\mathrm{Mpc}^{-1}$, corresponding to $\ell_0 = 29$. The values of σ are $\sigma = 2$ (top panel) $\sigma = 1.5$ (center panel), and $\sigma = 1$ (bottom panel), while we choose three different values of $\delta(\ell_0)$, as given in table 1: 0 (classical case, dotted lines), the observational upper bound from the numerical analysis (solid lines), and $\delta_{\max}$ (a-priori upper bound, dashed lines). Shaded regions are affected by cosmic variance.

where φ_{f} is the field value at the end of inflation determined by the condition $\epsilon_V \approx O(1)$. For the power-law potential (4.8) one has $\varphi_{\mathrm{f}} \approx n/\sqrt{2\kappa^2}$ and $N \approx n/(4\epsilon_V) - n/4$,
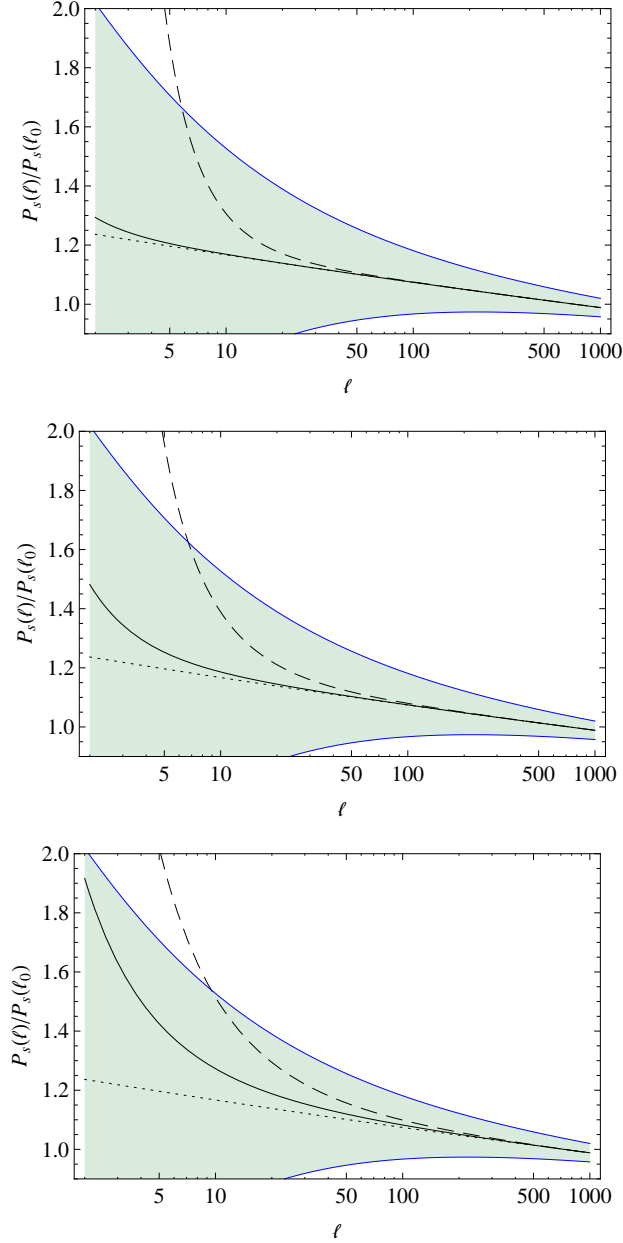
Figure 2: Primordial scalar power spectrum $\mathcal{P}_{\mathrm{s}}(\ell)$ for the case $n = 2$, with $\epsilon_V(k_0) = 0.009$ and the pivot wavenumber $k_0 = 0.05\,\mathrm{Mpc}^{-1}$, corresponding to $\ell_0 = 730$. The values of σ are $\sigma = 2$ (top panel), $\sigma = 1.5$ (center panel), and $\sigma = 1$ (bottom panel), while we choose three different values of $\delta(\ell_0)$, as given in table 1: 0 (classical case, dotted lines), the observational upper bound from the numerical analysis (solid lines), and $\delta_{\max}$ (a-priori upper bound, dashed lines). Shaded regions are affected by cosmic variance.

which gives

$$\epsilon_V \approx \frac{n}{4N + n}, \qquad 45 < N < 65\,. \tag{5.2}$$

The typical values of N for the perturbations relevant to the CMB anisotropies are

actually around $50 < N < 60$, but we have taken the wider range above. The comparison of this estimate with the experimental range of ϵ_V will determine the acceptance or exclusion of an inflationary model for a given n.

For the exponential potential (4.10) the slow-roll parameter ϵ_V is constant, which means that inflation does not end unless the shape of the potential changes after some epoch. In this case, we do not have constraints on ϵ_V coming from the information of the number of e-foldings in the observational range.

5.1 Quadratic potential

Let us study observational constraints in the case of the quadratic potential $V(\varphi) = V_0\varphi^2$.

5.1.1 $k_0 = 0.002$ **Mpc**$^{-1}$

We first take the pivot wavenumber $k_0 = 0.002$ Mpc^{-1} ($\ell_0 \approx 29$) used by the WMAP team [31]. In figure 3, the 2D posterior distributions of the parameters $\delta(k_0)$ and $\epsilon_V(k_0)$ are plotted for $n = 2$ and $\sigma = 2, 1.5, 0.5$. We have also run the code for other values of σ such as 1 and 3. The observational upper bounds on δ are given in table 1 for several different values of σ.

For $\sigma \lesssim 1$, the exponential factor $e^{-\sigma x}$ does not change rapidly with smaller values of $f_{\rm s,t}$, so that the LQC effect on the power spectra would not be very significant even if $\delta(k_0)$ was as large as $\epsilon_V(k_0)$. As we see in figure 1 (solid curve), if $\sigma = 0.5$ the LQC correction is constrained to be $\delta(k_0) < 0.27$ (95% CL), which exceeds the theoretical prior $\delta_{\rm max} = 0.26$. Since $\delta(k_0)$ is as large as 1 in such cases, the validity of the approximation $\delta(k_0) < \epsilon_V(k_0)$ to derive the power spectra is no longer reliable for $\sigma \lesssim 0.5$.

Looking at table 1, when $\sigma = 1$, the observational upper bound on $\delta(k_0)$ becomes of the same order as $\delta_{\rm max}$. For $\sigma \lesssim 1.5$ the effect of the LQC correction to the power spectrum becomes important on large scales relative to cosmic variance. For smaller σ the observational upper bound on $\delta(k_0) = \alpha_0\delta_{\rm Pl}(k_0)$ tends to be larger. When $\sigma = 1.5$ the LQC correction is constrained to be $\delta(k_0) < 1.7 \times 10^{-3}$ (95% CL), see figure 3. This is smaller than the theoretical prior $\delta_{\rm max} = 1.8 \times 10^{-2}$ by one order of magnitude.

The effect of cosmic variance is significant for $\sigma \gtrsim 1.5$. When $\sigma = 3$, the LQC correction is constrained to be $\delta(k_0) = \nu_0\delta_{\rm Pl}(k_0) < 4.3\times10^{-7}$ (95% CL). With respect to the prior $\delta_{\rm max} = 3.3 \times 10^{-4}$, the observational bound is smaller by three orders of magnitude. For $\sigma \gtrsim 3$ the power spectra grow very sharply for low multipoles, so that the upper bounds on $\delta(k_0)$ become smaller. Numerically it is difficult to deal with such rapidly changing power spectra.

For the sake of completeness, we should notice that the bounds plotted in Figs. 1 and 2 include input from several datasets, but the cosmic variance belt comes only from the CMB. Therefore, the medium-scale part of the cosmic-variance plots might
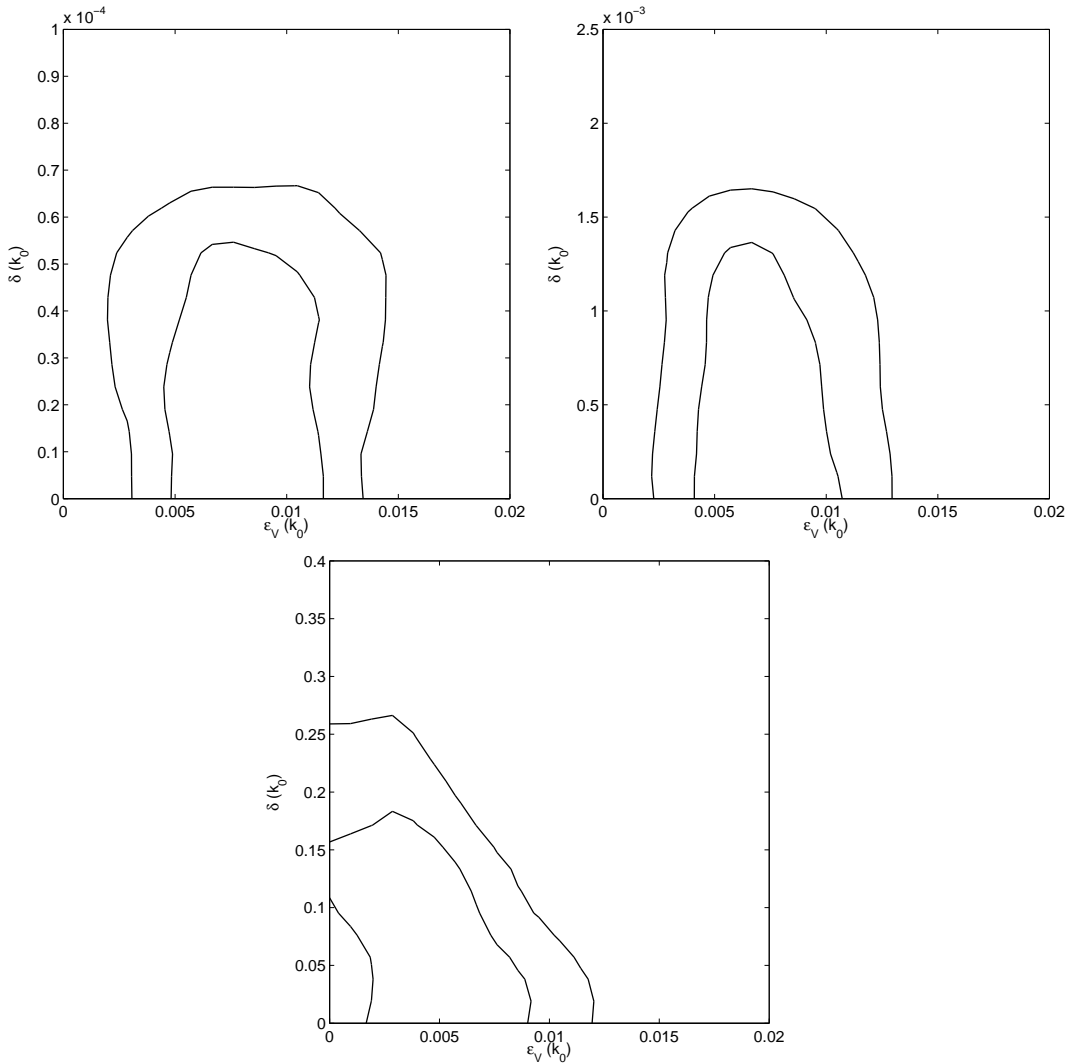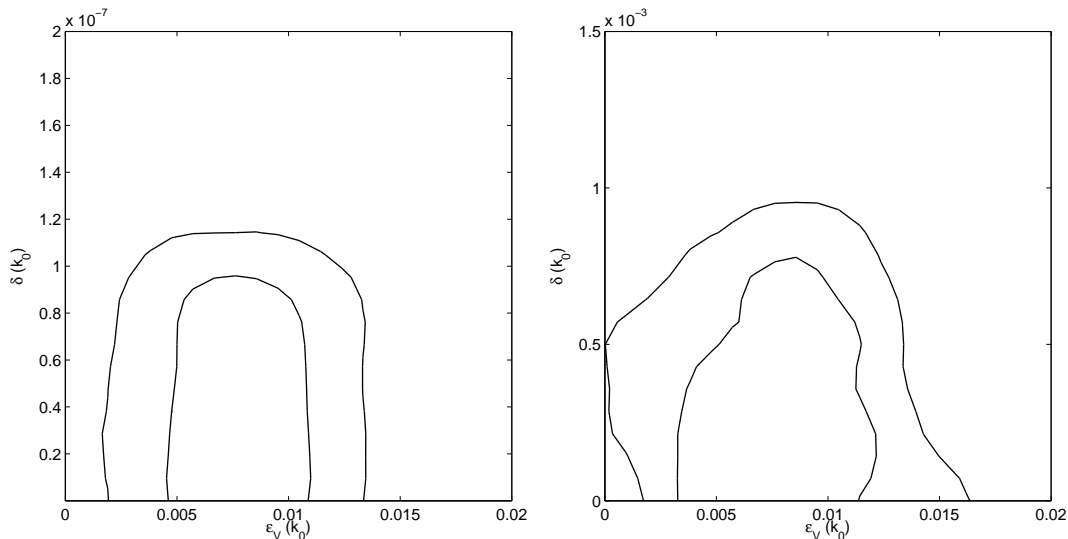
Figure 3: 2-dimensional marginalized distribution for the quantum-gravity parameter $\delta(k_0)$ and the slow-roll parameter $\epsilon_V(k_0)$ with the pivot $k_0 = 0.002$ Mpc^{-1} for $n = 2$, constrained by the joint data analysis of WMAP 7yr, LSS (including BAO), HST, SN Ia, and BBN. The values of σ are $\sigma = 2$ (top left panel), $\sigma = 1.5$ (top right panel), and $\sigma = 0.5$ (bottom panel). The internal and external lines correspond to the 68% and 95% confidence levels, respectively.

not give the full picture of the statistical limitations in this range, but we do not expect appreciable modifications from large-scale structure observations.

For $n = 2$, the theoretically constrained region (5.2) corresponds to $0.008 < \epsilon_V < 0.011$. As we see in figure 3, for $\sigma \gtrsim 0.5$, the probability distributions of ϵ_V are consistent with this range even in the presence of the LQC corrections. Hence, for the pivot wavenumber $k_0 = 0.002$ Mpc^{-1}, the quadratic potential is compatible with observations as in standard cosmology.

5.1.2 $k_0 = 0.05 \ \mathbf{Mpc}^{-1}$

Figure 4: 2-dimensional marginalized distribution for $n = 2$ with the pivot $k_0 = 0.05$ Mpc^{-1}. The values of σ are $\sigma = 2$ (left panel) and $\sigma = 1$ (right panel).

We proceed to the case of the pivot wavenumber $k_0 = 0.05$ Mpc^{-1} ($\ell_0 \approx 730$). From Eq. (4.17), the theoretical priors on δ_{max} for given σ are smaller than those corresponding to $k_0 = 0.002$ Mpc^{-1}. In figure 4 we plot the 2-dimensional posterior distribution of $\delta(k_0)$ and $\epsilon_V(k_0)$ for $n = 2$ and $\sigma = 2, 1$. When $\sigma = 2$, the observational upper limit is found to be $\delta(k_0) < 1.2 \times 10^{-7}$ (95% CL), which is two orders of magnitude smaller than the bound $\delta(k_0) < 6.8 \times 10^{-5}$ obtained for the pivot $k_0 = 0.002$ Mpc^{-1}. This comes from the fact that the choice of larger k_0 leads to more enhancement of power on large scales.

When $\sigma = 1$, we find the constraint $\delta(k_0) < 9.0 \times 10^{-4}$ (95% CL), which is about 1/3 of the theoretical prior $\delta_{\mathrm{max}} = 2.7 \times 10^{-3}$. From table 1, we see that the observational limit of δ for $\sigma = 0.5$ exceeds δ_{max}. Hence, our combined slow-roll/δ_{Pl} truncation is no longer trustable for $\sigma \lesssim 0.5$, as it happens for $k_0 = 0.002$ Mpc^{-1}.

From figure 4 we find that the theoretically allowed range of ϵ_V ($0.008 < \epsilon_V < 0.011$) is consistent with its observational constraints. The different choice of k_0 affects the upper bounds on $\delta(k_0)$, but the basic property of the LQC effect on the power spectra is similar. The quadratic inflaton potential can be consistent with the combined observational constraints even in the presence of the LQC corrections, independent of the values of k_0 relevant to the CMB anisotropies.

5.2 Quartic potential

Let us proceed to the case of the quartic potential $V(\varphi) = V_0 \varphi^4$. Numerically, we find that the observational upper bounds on $\delta(k_0)$ for given σ and k_0 are similar to those
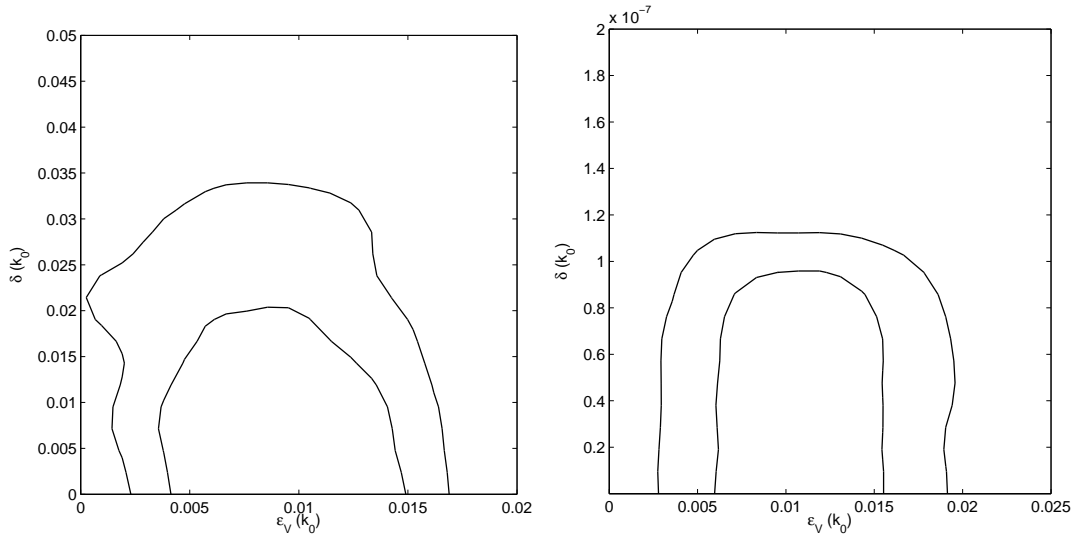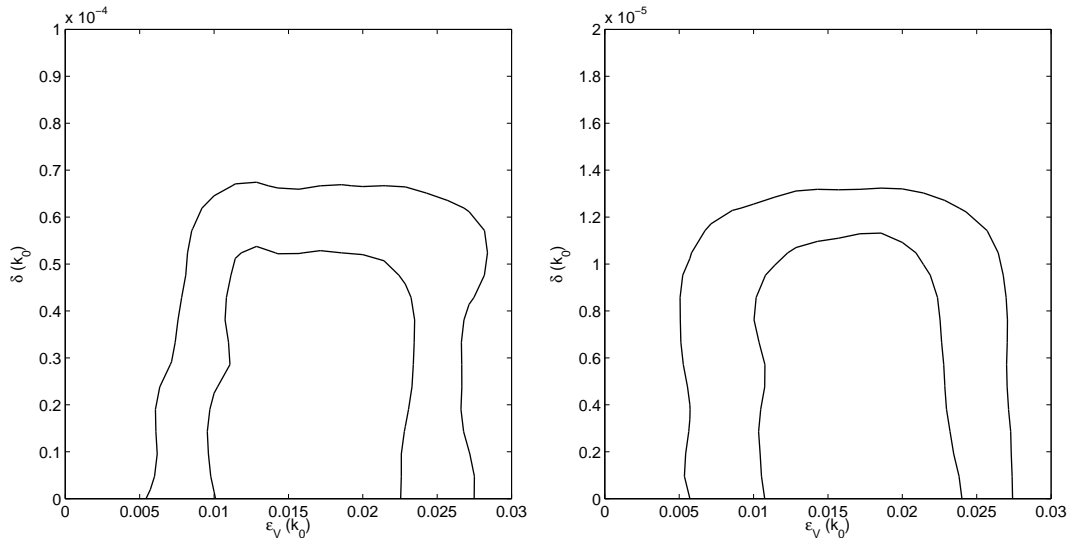
Figure 5: 2-dimensional marginalized distribution for $n = 4$ in the two cases: (i) $\sigma = 1$ and $k_0 = 0.002$ Mpc^{-1} (left panel) and (ii) $\sigma = 2$ and $k_0 = 0.05$ Mpc^{-1} (right panel).

for the quadratic potential. In the top panel of figure 5 we show the 2-dimensional distribution for $\sigma = 1$ with the pivot wavenumber $k_0 = 0.002$ Mpc^{-1}. The LQC correction is constrained to be $\delta(k_0) < 3.4 \times 10^{-2}$ (95 % CL), which is similar to the bound $\delta(k_0) < 3.5 \times 10^{-2}$ for $n = 2$ (see table 1). The bottom panel of figure 5 corresponds to the posterior distribution for $\sigma = 2$ with $k_0 = 0.05$ Mpc^{-1}, in which case $\delta(k_0) < 1.1 \times 10^{-7}$ (95 % CL). Since the LQC correction given in Eq. (4.15) does not depend on the values of n, the above property of n-independence can be expected. For larger σ and k_0 the upper bounds on $\delta(k_0)$ tend to be smaller.

From Eq. (5.2), the values of ϵ_V related with the CMB anisotropies fall in the range $0.015 < \epsilon_V < 0.022$. For $\sigma = 1$ and $k_0 = 0.002$ Mpc^{-1}, this range is outside the 1σ likelihood contour. In particular, for $N < 58$, this model is excluded at the 95% confidence level. For $\sigma = 2$ the observationally allowed region of ϵ_V is slightly wider than that for $\sigma = 1$. However, as we see in the lower panel of figure 5, this model is still under an observational pressure. Numerically we have confirmed that the bounds on $\epsilon_V(k_0)$ are insensitive to the choice of k_0. Hence the quartic potential is in tension with observations even in the presence of the LQC corrections.

5.3 Exponential potentials

Finally, we study the case of exponential potentials. In figure 6 we show the 2-dimensional posterior distribution for (i) $\sigma = 2$ and $k_0 = 0.002$ Mpc^{-1} and (ii) $\sigma = 1.5$ and $k_0 = 0.05$ Mpc^{-1}. The observational upper limits on the LQC corrections for the cases (i) and (ii) are $\delta(k_0) < 6.8 \times 10^{-5}$ and $\delta(k_0) < 1.3 \times 10^{-5}$, respectively, which are similar to those for $n = 2$ with same values of σ. Hence, for given values of σ and k_0, the effect of the LQC corrections to the power spectra is practically independent

Figure 6: 2-dimensional marginalized distribution for the exponential potential $V(\varphi) = V_0 e^{-\kappa\lambda\varphi}$ in the two cases: (i) $\sigma = 2$ and $k_0 = 0.002$ Mpc^{-1} (left panel) and (ii) $\sigma = 1.5$ and $k_0 = 0.05$ Mpc^{-1} (right panel).

of the choice of the inflaton potentials.

On the other hand, the observational constraints on the slow-roll parameter depend on the potential. In figure 6 we find that the observationally allowed values of $\epsilon_V(k_0)$ are in the range $0.005 < \epsilon_V(k_0) < 0.27$ (95 % CL) for two different choices of k_0. The maximum value of $\epsilon_V(k_0)$ is larger than that for $n = 2$ and $n = 4$. Since inflation does not end for exponential potentials, one cannot estimate the range of the slow-roll parameter relevant to the CMB anisotropies. Hence one needs to find a mechanism of a graceful exit from inflation in order to address this issue properly.

6. Conclusions

In the presence of the inverse-volume corrections in LQC, we have provided the explicit forms of the scalar and tensor spectra convenient to confront inflationary models with observations. Even if the LQC corrections are small at the background level, they can significantly affect the runnings of spectral indices. We have consistently included the terms of order higher than the scalar/tensor runnings. Inverse-volume corrections generally lead to an enhancement of the power spectra at large scales.

Using the recent observational data of WMAP 7yr combined with LSS, HST, SN Ia, and BBN we have placed constraints on the power-law potentials $V(\varphi) = V_0\varphi^n$ ($n = 2, 4$) as well as the exponential potentials $V(\varphi) = V_0 e^{-\kappa\lambda\varphi}$. The inflationary observables (the scalar and tensor power spectra $\mathcal{P}_s$, $\mathcal{P}_t$ and the tensor-to-scalar ratio r) can be written in terms of the slow-roll parameter $\epsilon_V = (V_{,\varphi}/V)^2/(2\kappa^2)$ and the normalized LQC correction term δ. We have carried out a likelihood analysis by

varying these two parameters as well as other cosmological parameters for two pivot wavenumbers k_0 (0.002 Mpc^{-1} and 0.05 Mpc^{-1}).

The observational upper bounds on $\delta(k_0)$ tend to be smaller for larger values of k_0. In table 1 we listed the observational upper limits on $\delta(k_0)$ as well as the theoretical priors δ_{max} for the quadratic potential $V(\varphi) = V_0\varphi^2$ with a number of different values of the quantum gravity parameter σ (which is related to δ as $\delta \propto a^{-\sigma}$). For larger σ, we find that $\delta(k_0)$ needs to be suppressed more strongly to avoid the significant enhancement of the power spectra at large scales. When $\sigma \lesssim 0.5$ the observational upper limits of $\delta(k_0)$ exceed the theoretical prior δ_{max}, which means that the expansion in terms of the inverse-volume corrections can be trustable for $\sigma \gtrsim 0.5$.

As we see in Figs. 3-6 and in table 1, the observational upper bounds on $\delta(k_0)$ for given k_0 and σ are practically independent of the choice of the inflaton potentials. This property comes from the fact that the LQC correction for the wavenumber k is approximately given by $\delta(k) = \delta(k_0)(k_0/k)^\sigma$, which only depends on k_0 and σ. On the other hand the constraints on the slow-roll parameter ϵ_V are different depending on the choice of the inflaton potentials. We have found that the quadratic potential is consistent with the current observational data even in the presence of the LQC corrections, but the quartic potential is under an observational pressure. For the exponential potentials the larger values of ϵ_V are favored compared to the power-law potentials. However, the exponential potentials are not regarded as a realistic scenario unless there is a graceful exit from inflation.

If we compare the observational upper bounds with the theoretical lower bounds discussed in section 2, we can see that estimates of these parameters are separated by at most a few orders of magnitude, much less than is usually expected for quantum gravity. By accounting for fundamental spacetime effects that go beyond the usual higher-curvature corrections, quantum gravity thus comes much closer to falsifiability than often granted. It is of interest to see how the future high-precision observations such as PLANCK will constrain the LQC correction as well as the slow-roll parameters. Even in the case where the quadratic potential were not favored in future observations, it would be possible that the small-field inflationary models be consistent with the data. For these general inflaton potentials, the effect of inverse-volume corrections on the CMB anisotropies should be similar to that studied in this paper.

ACKNOWLEDGEMENTS

References

[1] M. Bojowald and G.M. Hossain, *Cosmological vector modes and quantum gravity effects, Class. Quant. Grav.* **24** (2007) 4801 [arXiv:0709.0872].

[2] M. Bojowald and G.M. Hossain, *Loop quantum gravity corrections to gravitational wave dispersion, Phys. Rev.* **D 77** (2008) 023508 [arXiv:0709.2365].

[3] J. Mielczarek, T. Cailleteau, A. Barrau and J. Grain, *Anomaly-free vector perturbations with holonomy corrections in loop quantum cosmology,* arXiv:1106.3744.

[4] M. Bojowald, G.M. Hossain, M. Kagan and S. Shankaranarayanan, *Anomaly freedom in perturbative loop quantum gravity, Phys. Rev.* **D 78** (2008) 063547 [arXiv:0806.3929].

[5] M. Bojowald, G.M. Hossain, M. Kagan and S. Shankaranarayanan, *Gauge invariant cosmological perturbation equations with corrections from loop quantum gravity, Phys. Rev.* **D 79** (2009) 043505 [arXiv:0811.1572];

Erratum-ibid: **D 82** (2010) 109903(E).

[6] E.J. Copeland, D.J. Mulryne, N.J. Nunes and M. Shaeri, *The gravitational wave background from super-inflation in Loop Quantum Cosmology, Phys. Rev.* **D 79** (2009) 023508 [arXiv:0810.0104].

[7] G. Calcagni and G.M. Hossain, *Loop quantum cosmology and tensor perturbations in the early universe, Adv. Sci. Lett.* **2** (2009) 184 [arXiv:0810.4330].

[8] M. Bojowald and G. Calcagni, *Inflationary observables in loop quantum cosmology, JCAP* **03** (2011) 032 [arXiv:1011.2779].

[9] M. Bojowald, G. Calcagni and S. Tsujikawa, *Observational constraints on loop quantum cosmology,* arXiv:1101.5391.

[10] M. Bojowald, *Inflation from quantum geometry, Phys. Rev. Lett.* **89** (2002) 261301 [arXiv:gr-qc/0206054];

S. Tsujikawa, P. Singh and R. Maartens, *Loop quantum gravity effects on inflation and the CMB, Class. Quant. Grav.* **21** (2004) 5767 [arXiv:astro-ph/0311015];

M. Bojowald, J.E. Lidsey, D.J. Mulryne, P. Singh and R. Tavakol, *Inflationary cosmology and quantization ambiguities in semiclassical loop quantum gravity, Phys. Rev.* **D 70** (2004) 043530 [arXiv:gr-qc/0403106];

G.M. Hossain, *Primordial density perturbation in effective loop quantum cosmology, Class. Quant. Grav.* **22** (2005) 2511 [arXiv:gr-qc/0411012];

G. Calcagni and M. Cortês, *Inflationary scalar spectrum in loop quantum cosmology, Class. Quant. Grav.* **24** (2007) 829 [arXiv:gr-qc/0607059];

E.J. Copeland, D.J. Mulryne, N.J. Nunes and M. Shaeri, *Super-inflation in loop quantum cosmology, Phys. Rev.* **D 77** (2008) 023510 [arXiv:0708.1261];

M. Shimano and T. Harada, *Observational constraints on a power spectrum from super-inflation in loop quantum cosmology*, Phys. Rev. **D 80** (2009) 063538 [arXiv:0909.0334].

[11] A. Barreau *et al.*, private communication.

[12] J. Mielczarek, *Gravitational waves from the Big Bounce*, JCAP **11** (2008) 011 [arXiv:0807.0712].

[13] J. Grain and A. Barrau, *Cosmological footprints of loop quantum gravity*, Phys. Rev. Lett. **102** (2009) 081301 [arXiv:0902.0145].

[14] M. Bojowald, *Large scale effective theory for cosmological bounces*, Phys. Rev. **D 74** (2007) 081301 [arXiv:gr-qc/0608100].

[15] M. Bojowald, W. Nelson, D. Mulryne and R. Tavakol, *The high-density regime of kinetic-dominated loop quantum cosmology*, Phys. Rev. **D 82** (2010) 124055 [arXiv:1004.3979].

[16] A. Ashtekar, T. Pawlowski and P. Singh, *Quantum nature of the big bang: improved dynamics*, Phys. Rev. **D 74** (2006) 084003 [arXiv:gr-qc/0607039].

[17] A. Ashtekar, J. Baez, A. Corichi and K. Krasnov, *Quantum geometry and black hole entropy*, Phys. Rev. Lett. **80** (1998) 904 [arXiv:gr-qc/9710007].

[18] A. Ashtekar, J.C. Baez, and K. Krasnov, *Quantum geometry of isolated horizons and black hole entropy*, Adv. Theor. Math. Phys. **4** (2000) 1 [arXiv:gr-qc/0005126].

[19] T. Thiemann, *Quantum spin dynamics (QSD)*, Class. Quant. Grav. **15** (1998) 839 [arXiv:gr-qc/9606089].

[20] T. Thiemann, *QSD 5: Quantum gravity as the natural regulator of matter quantum field theories*, Class. Quant. Grav. **15** (1998) 1281 [arXiv:gr-qc/9705019].

[21] M. Bojowald and A. Skirzewski, *Effective equations of motion for quantum systems*, Rev. Math. Phys. **18** (2006) 713 [arXiv:math-ph/0511043].

[22] M. Bojowald, B. Sandhöfer, A. Skirzewski and A. Tsobanjan, *Effective constraints for quantum systems*, Rev. Math. Phys. **21** (2009) 111 [arXiv:0804.3365].

[23] M. Bojowald and A. Tsobanjan, *Effective constraints for relativistic quantum systems*, Phys. Rev. **D 80** (2009) 125008 [arXiv:0906.1772].

[24] M. Bojowald, *Inverse scale factor in isotropic quantum geometry*, Phys. Rev. **D 64** (2001) 084018 [arXiv:gr-qc/0105067].

[25] M. Bojowald, H. Hernández, M. Kagan and A. Skirzewski, *Effective constraints of loop quantum gravity*, Phys. Rev. **D 75** (2007) 064022 [arXiv:gr-qc/0611112].

[26] M. Bojowald, *egenerate configurations, singularities and the non-Abelian nature of loop quantum gravity, Class. Quant. Grav.* **23** (2006) 987 [arXiv:gr-qc/0508118].

[27] J.E. Lidsey, A.R. Liddle, E.W. Kolb, E.J. Copeland, T. Barreiro and M. Abney, *Reconstructing the inflation potential: an overview, Rev. Mod. Phys.* **69** (1997) 373 [arXiv:astro-ph/9508078];

B.A. Bassett, S. Tsujikawa and D. Wands, *Inflation dynamics and reheating, Rev. Mod. Phys.* **78** (2006) 537 [arXiv:astro-ph/0507632].

[28] U. Seljak and M. Zaldarriaga, *A Line of sight integration approach to cosmic microwave background anisotropies, Astrophys. J.* **469** (1996) 437 [arXiv:astro-ph/9603033].

[29] *http://cosmologist.info/cosmomc/*

[30] H. V. Peiris *et al.* [WMAP Collaboration], *First year Wilkinson Microwave Anisotropy Probe (WMAP) observations: implications for inflation, Astrophys. J. Suppl.* **148** (2003) 213 [arXiv:astro-ph/0302225].

[31] E. Komatsu *et al.* [WMAP Collaboration], *Seven-Year Wilkinson Microwave Anisotropy Probe (WMAP) observations: cosmological interpretation, Astrophys. J. Suppl.* **192** (2011) 18 [arXiv:1001.4538].

[32] S.M. Leach and A.R. Liddle, *Constraining slow-roll inflation with WMAP and 2dF, Phys. Rev.* **D 68** (2003) 123508 [arXiv:astro-ph/0306305].

[33] M. Cortês, A.R. Liddle and P. Mukherjee, *On what scale should inflationary observables be constrained?, Phys. Rev.* **D 75** (2007) 083520 [arXiv:astro-ph/0702170].

[34] A.D. Linde, *Chaotic inflation, Phys. Lett.* **B 129** (1983) 177.

[35] F. Lucchin and S. Matarrese, *Power law inflation, Phys. Rev.* **D 32** (1985) 1316.

[36] J.R. Bond and G. Efstathiou, *The statistics of cosmic background radiation fluctuations, Mon. Not. R. Astron. Soc.* **226** (1987) 655;

L. Knox and M.S. Turner, *Detectability of tensor perturbations through CBR anisotropy, Phys. Rev. Lett.* **73** (1994) 3347 [arXiv:astro-ph/9407037].

[37] B.A. Reid *et al.*, *Cosmological constraints from the clustering of the Sloan Digital Sky Survey DR7 luminous red galaxies, Mon. Not. R. Astron. Soc.* **404** (2010) 60 [arXiv:0907.1659].

[38] A.G. Riess *et al.*, *A redetermination of the Hubble constant with the Hubble Space Telescope from a differential distance ladder, Astrophys. J.* **699** (2009) 539 [arXiv:0905.0695].

[39] M. Kowalski *et al.* [Supernova Cosmology Project Collaboration], *Improved cosmological constraints from New, Old and Combined Supernova datasets,* *Astrophys. J.* **686** (2008) 749 [arXiv:0804.4142].

[40] S. Burles and D. Tytler, *The Deuterium abundance towards Q1937-1009, Astrophys. J.* **499** (1998) 699 [arXiv:astro-ph/9712108].